

LIISA LANG

Baculate shell structure in Early Palaeozoic
linguliform brachiopods



LIISA LANG

Baculate shell structure in Early Palaeozoic
linguliform brachiopods



Department of Geology, Institute of Ecology and Earth Sciences, Faculty of Science and Technology, University of Tartu, Estonia.

This dissertation was accepted for the commencement of the degree of Doctor of Philosophy in Geology at the University of Tartu on 18th May, 2015 by the Scientific Council of the Institute of Ecology and Earth Sciences, University of Tartu.

Supervisors: Prof. Tõnu Meidla and Dr. Ivar Puura,
Department of Geology, University of Tartu, Estonia

Opponent: Prof. Lars Holmer, Department of Earth Sciences,
Uppsala University, Sweden

This thesis will be defended at the University of Tartu, Estonia, Ravila 14A, room 1019, on the 22nd of September 2015 at 14:15.

Publication of this thesis is granted by the Institute of Ecology and Earth Sciences, University of Tartu.

ISSN 1406-2658
ISBN 978-9949-32-903-8 (print)
ISBN 978-9949-32-904-5 (pdf)

Copyright: Liisa Lang, 2015

University of Tartu Press
www.tyk.ee

CONTENTS

LIST OF ORIGINAL PUBLICATIONS	6
ABBREVIATIONS	7
THESIS AT A GLANCE	8
1. INTRODUCTION	10
2. STRUCTURE AND COMPOSITION OF LINGULIFORM BRACHIOPOD SHELLS	12
2.1. Modern linguliforms	12
2.1.1. Shell composition	12
2.1.2. Nanostructures	13
2.1.3. Microstructures	14
2.2. Fossil linguliforms	16
2.2.1. Shell composition	16
2.2.2. Nanostructures	16
2.2.3. (Baculate) microstructures	16
3. MATERIAL	18
4. METHODS	19
5. RESULTS	21
5.1. Baculate shell structure	21
5.1.1. General notes on preservation	21
5.1.2. Nanofibrils	24
5.2. Chemical composition of valve apatite	25
6. DISCUSSION	29
6.1. Shell apatite phases and their origin	29
6.2. Nature and origin of nanofibrils	32
6.3. Variation in baculate shell structures	35
6.4. Diagenesis	38
7. CONCLUSIONS	43
ACKNOWLEDGEMENTS	45
REFERENCES	46
SUMMARY IN ESTONIAN	53
PUBLICATIONS	57
CURRICULUM VITAE	109
ELULOOKIRJELDUS	111

LIST OF ORIGINAL PUBLICATIONS

This thesis is based on the following published papers, which are referred to in the text by their Roman numerals. The papers are reprinted by kind permission of the publishers.

- I **Lang, L.**, Puura, I. 2009: Systematic position, distribution, and shell structure of the Devonian linguloid brachiopod *Bicarinatina bicarinata* (Kutorga, 1837). Estonian Journal of Earth Sciences, 58(1), 63–70. Copyright © 2009 Estonian Academy Publishers.
- II **Lang, L.**, Uibopuu, E., Puura, I. 2011: Nanostructures in Palaeozoic linguloid brachiopods. Memoirs of the Association of Australasian Palaeontologists, 41, 359–366. Copyright © 2011 Association of Australasian Palaeontologists.
- III **Lang, L.**, Puura, I. 2013: Phosphatized organic nanostructures in the Cambrian linguloid brachiopod *Ungula inornata* (Mickwitz). Estonian Journal of Earth Sciences, 62(3), 121–130. Copyright © 2013 Estonian Academy Publishers.
- IV **Lang, L.**, Kirsimäe, K., Vahur, S. 2015: Diagenetic fate of bioapatite in linguliform brachiopods: multiple apatite phases in shells of Cambrian lingulate brachiopod *Ungula ingraca* (Eichwald). Lethaia (in press), DOI: 10.1111/let.12127. Copyright © 2015 Lethaia Foundation. Published by John Wiley & Sons Ltd. (electronic version available at <http://onlinelibrary.wiley.com/doi/10.1111/let.12127/abstract>)

Author's contribution:

- Paper I:** The author took part in fieldwork, studied the palaeontological collections of *Bicarinatina* specimens and was responsible for sample measurements, photography and preparation for scanning electron microscopy (SEM) studies, data interpretation and preparing the manuscript.
- Paper II:** The author was responsible for SEM studies, data interpretation and the writing of the manuscript.
- Paper III:** The author was responsible for SEM studies, data interpretation and the writing of the manuscript.
- Paper IV:** The author was responsible for planning the research and fieldwork, preparing the samples, analysing and interpreting of various geochemical data, implementing analytical SEM studies, and the writing of the manuscript.

ABBREVIATIONS

SEM	scanning electron microscopy
SE	secondary electron (regime of SEM)
BSE	backscattered electron (regime of SEM)
EDS	energy dispersive spectroscopy
FTIR	Fourier transform infrared (microscopy)
ATR	Attenuated total reflectance (mode of FTIR)
XRD	X-ray diffraction

THESIS AT A GLANCE

Paper I	Systematic position, distribution, and shell structure of the Devonian linguloid brachiopod <i>Bicarinatina bicarinata</i> (Kutorga, 1837)
Aim	To clarify the systematic status of <i>Bicarinatina bicarinata</i> (Kutorga) and related species reported from the East Baltic by revision of the original collection of Viktors Gravitis at the Latvian Museum of Natural History and to give the first description of the shell microstructure of this species.
Specimens	Topotypic collection of <i>Lingula bicarinata</i> (2 specimens); original collection of Devonian linguloids in Latvia (~30 samples); material collected from Estonia (~20 samples); new material collected by authors.
Methods	Mg-coated photography, valve measurements, SEM (BSE), EDS.
Results	The studied valve is about 70–100 µm thick, very even in thickness. The bacula are thicker, 0.25–0.5 µm across, close to valve exterior than those close to the interior of the valve. Compact laminae appear to be thicker than baculate laminae close to the interior of the valve.
Conclusions	The genus <i>Bicarinatina</i> includes four species: <i>Bicarinatina bicarinata</i> , <i>Liralingua indicis</i> , <i>Liralingua wilsoni</i> , and <i>Bicarinatina kongakutensis</i> . None of the eight new species of the genus <i>Bicarinatina</i> described by Gravitis (1981) can be considered as valid. Occurrence of <i>B. bicarinata</i> : Estonia, Latvia, NW Russia. The very fine bacula observed in <i>B. bicarinata</i> give evidence of exclusive preservation.

Paper II	Nanostructures in Palaeozoic linguloid brachiopods
Aim	To describe the exceptional preservation of baculate structure in Palaeozoic linguloid brachiopods.
Specimens	Illustrated specimens: 1 valve of <i>Bicarinatina bicarinata</i> (Devonian, Estonia); 1 valve of <i>Obolus ruchini</i> (Cambrian, NW Russia).
Methods	Untreated and uncoated fracture sections of valves studied with SEM (BSE), EDS.
Results	Delicate phosphatized fibril-like nanostructures responsible for the formation of the bacula have been observed. <i>B. bicarinata</i> – nanofibril diameter 150 nm. <i>O. ruchini</i> – preservation ‘windows’ with nanofibrils less than 200 nm in diameter.
Conclusions	Phosphatized fibril-like nanostructures are found in Palaeozoic linguloid brachiopod shells and such kind of preservation may be more common than previously realized. These fibrils (at least part of them) may have been non-mineralized <i>in vivo</i> and are preserved due to rapid phosphatization. Such structures can be best observed during the study of untreated and uncoated fracture surfaces with low-vacuum SEM in the back-scattered regime. The first published report of the preservation of flexible nanofibrils of linguloid brachiopods in the fossil state.

Paper III	Phosphatized organic nanostructures in the Cambrian linguloid brachiopod <i>Ungula inornata</i> (Mickwitz)
Aim	To describe flexible nanofibrils in the Cambrian linguloid brachiopod <i>Ungula inornata</i> .
Specimens	<i>Ungula inornata</i> . Structure – 1; other specimens – 3.
Methods	SEM, concurrent SE and BSE regimes; untreated and uncoated fracture sections.
Results	Different preservation of baculate structures, nanofibrils.
Conclusions	Nanofibrils are relevant structural units in the hierarchical structure of lingulate brachiopods with baculate shell structure. They are preserved by instant post-mortem precipitation of apatite. The shell structure of <i>U. inornata</i> is most similar to those of the other species of the genus <i>Ungula</i> Pander and the species of the genus <i>Obolus</i> Eichwald. In many cases, especially at higher magnifications, BSE images bearing compositional information are more informative than SE images for observing nanostructures and shell structure in general. However, both types of images complement each other.

Paper IV	Diagenetic fate of bioapatite in linguliform brachiopods: multiple apatite phases in shells of Cambrian lingulate brachiopod <i>Ungula ingrlica</i> (Eichwald)
Aim	To study the chemical variability of apatite in the fossil lingulate brachiopod <i>Ungula ingrlica</i> ; to localize different apatite phases within the shell and understand apatite diagenetic replacement and/or recrystallization patterns with respect to the baculate stratiform structure of these brachiopods.
Specimens	<i>Ungula ingrlica</i> , XRD – 10 valves; ATR-FTIR – 2 valves; SEM – 2 valves; <i>Lingula anatina</i> – ATR-FTIR (1 valve).
Methods	ATR-FTIR (the first employment of ATR mapping on fossil linguliform brachiopod shells), SEM-EDS, XRD; polished fracture sections of valves; SEM (SE) Pt-coated.
Results	Two apatite phases, one can be associated with compact laminae, the other with baculate laminae. In compact laminae: apatite crystallite size similar to crystallite size of modern lingulids; apatite chemistry: less carbonate anions and fluoride, also less calcium and more Na and Mg; XRD lattice parameter values are probably higher. Apatite in baculate laminae – rich in carbonate anions and fluorine, crystals bigger and needle-like; XRD lattice parameter values likely lower.
Conclusions	Apatite phase in baculate laminae is mostly authigenic, while apatite in compact laminae can be interpreted as early diagenetically recrystallized skeletal apatite. If some original features are preserved in brachiopod shell apatite, these are most likely found in the (central parts of) compact laminae.

I. INTRODUCTION

Linguliform (subphylum Linguliformea) brachiopods are benthic marine invertebrates that secrete their bivalved shells of Ca-phosphate mineral apatite (Williams *et al.* 1996; Williams *et al.* 2000; Holmer & Popov 2007). This characteristic differentiates them from most of other marine invertebrates, including the majority of other brachiopod taxa that have their mineralized parts made of Ca-carbonate, whereas apatite is a typical skeletal mineral in vertebrates. In addition to that, linguliform brachiopods have a long geologic history. They are known since at least the Late Terreneuvian (Bassett *et al.* 1999; Ushatinskaya 2008) and have survived until today. Linguliform brachiopods are, thus, suitable objects for the study of the evolutionary relationships between brachiopods and related clades (e.g. Balthasar & Butterfield 2008; Holmer *et al.* 2008; Balthasar *et al.* 2009; Larsson *et al.* 2014), and for revealing the biomineralization patterns and evolution of mineralized skeletons in organisms (e.g. Knoll 2003; Kouchinsky *et al.* 2012; Zabini *et al.* 2012). Furthermore, linguliform brachiopods have been used to gain palaeoclimatic information stored in their shell apatite in the brachiopod lifetime (e.g. Léquyer *et al.* 1996, 1998; Wenzel *et al.* 2000; Bassett *et al.* 2007). All these studies, however, require the understanding of the taphonomic changes in biominerals and mineralized structures.

The shell of linguliform brachiopods is typically composed of alternating compact and porous laminae. Specific arrangement of apatite in porous laminae is commonly used to define the shell microstructure. Several types of microstructures have been defined in linguliform brachiopods (Williams & Holmer 1992; Cusack *et al.* 1999; Williams & Cusack 1999; 2007; Williams *et al.* 2004; Holmer *et al.* 2008; Streng *et al.* 2008) which are important in brachiopod phylogenesis (e.g. Cusack *et al.* 1999). Two main types of microstructures, characteristic of the secondary shell of Palaeozoic linguliform brachiopods, are columnar and baculate symmetrical structures (Cusack *et al.* 1999; Williams & Cusack 1999; 2007). Columnar structure occurs in acrotretoids, but also in some Cambrian linguloids, e.g. *Lingulellotreta* (Williams & Cusack 1999), *Kyrshabaktella* (Skovsted & Holmer 2006), *Canalilatus? simplex* and *Eoobolus? sp. aff. E. priscus* (Streng *et al.* 2008).

The term *baculate structure* was introduced by Lars E. Holmer in 1989 to describe small apatitic rods called *bacula* (Latin: *baculum*– small rod, pl. *bacula*) that form a trellised (criss-cross) pattern in the organic-rich (porous) laminae of the secondary shell of some modern and fossil linguliform brachiopods. This type of shell structure has previously been noticed by Iwata (1982) as mineralized fibrils in a lattice-like manner (*Glottidia*, *Discinisca*) and Watabe & Pan (1984) as crystalline rods made of aggregates of spherulites often forming ‘X’-figures (*Glottidia*) and later described in other fossil and modern linguliforms. Baculate shell structure has a wide stratigraphic range and is supposed to be characteristic of most of fossil linguloids (Cusack *et al.* 1999),

known since at least Cambrian Epoch 2 (Skovsted & Peel 2010). This type of microstructure is also common in modern linguliforms, which allows comparison between fossil and recent linguloids (e.g. Cusack & Williams 1996). However, only a few studies address the details of baculate shell structure (e.g. Cusack *et al.* 1999; Williams & Cusack 1999) and the preservation of primary baculate shell structures (Cusack & Williams 1996; Williams & Cusack 1997).

The full range of diagenetic changes in fossil shells should also be considered to assess the usefulness and reliability of these apatitic remains as proxies for palaeoenvironmental or ecological information (Trueman 2013). The use of linguliform brachiopods or any other bioapatitic fossil as palaeoenvironmental proxies is, however, considered to be hampered by vital effects on phosphate secretion and significant diagenetic alteration of bioapatite (e.g. Lécuyer *et al.* 1996, 1998; Wenzel *et al.* 2000; Rodland *et al.* 2003; Bassett *et al.* 2007; Tütken *et al.* 2012). Furthermore, two apatite phases have been detected in fossil brachiopod shells using X-ray diffraction (XRD) analyses of bulk shell material (Nemliher *et al.* 2004). These phases suggest that shell microstructures are composed of a mixture of apatites precipitated and/or recrystallized in different diagenetic conditions and possibly at different rates and times. Differences between these apatite phases and their specific locations in shell structure are not known. An intriguing and important question is whether some parts of the brachiopod shells are chemically less altered than others and could potentially be used for the acquisition of reliable palaeoenvironmental-geochemical data.

The **overall aim** of this thesis is to study the structural and chemical variability of fossil linguliform brachiopod shells. The shell structure of three Early Palaeozoic linguloid species, *Ungula inornata* (Mickwitz, 1896), *Obolus ruchini* Khazanovitch *et* Popov, 1984 (in Khazanovitch *et al.* 1984) and *Bicarinatina bicarinata* (Kutorga, 1837), was studied in detail and the chemical variability of shell apatite in the valves of *Ungula ingraca* (Eichwald 1829) was mapped for developing a scenario of diagenetic changes in shells of linguliform brachiopods.

The **specific aims** of this thesis are:

- to reveal the preservational patterns of baculate shell structures in fossil linguliform brachiopods in order to understand the range of variations in this structure type;
- to analyse the relationships between different diagenetic/preservation states of baculate shell structures in linguliform shells in order to understand how baculate structures were formed in Early Palaeozoic linguliforms;
- to characterize apatite phases in linguliform brachiopod shells in order to understand apatite diagenetic replacement and/or recrystallization patterns in fossil brachiopod shells and to estimate the extent of diagenetic changes;
- to develop a generalized scenario of shell diagenesis and assess the usefulness of the apatite composition in fossil linguliform shells for palaeoenvironmental interpretations.

2. STRUCTURE AND COMPOSITION OF LINGULIFORM BRACHIOPOD SHELLS

Only a limited number of species of six genera of linguliforms are living today (Table 1). Modern linguliform shells were used for comparison, in order to interpret the microstructure and shell composition of Early Palaeozoic linguliforms.

Table 1. Families, genera and number of species of extant linguliform brachiopods (after Emig *et al.* 2013, 2015; data about shell structures from Iwata 1982; Williams *et al.* 1992, 1994, 1998; Cusack *et al.* 1999; Williams & Cusack 1999, 2007).

Family	Genus (No. of species)	Shell structure
Lingulidae	<i>Lingula</i> (7)	Botryoidal/virgose
	<i>Glottidia</i> (5)	Baculate (lenses)
Discinidae	<i>Pelagodiscus</i> (1)	Baculate (incipient)
	<i>Discina</i> (1)	Baculate
	<i>Discinisca</i> (5)	Baculate (only in ventral valve)
	<i>Discradisca</i> (6)	Baculate

2.1. Modern linguliforms

2.1.1. Shell composition

Shells of modern linguliforms are composed of various apatite aggregates in organic matrix. The organic part of the shell consists of sulphated glycosaminoglycans (GAGs), more than 10 proteins and β -chitin (Williams 1997; Williams & Cusack 1999, 2007); in addition also collagen has been found in the shell of *Lingula* (Williams *et al.* 1994). Glycosaminoglycans occur in the shell as elastic isotropic gel-like masses that are mainly featureless (Williams *et al.* 1994), but also as discrete bodies (sheets, ellipsoidal inclusions) (Williams *et al.* 1998). The other constituents are mainly fibrous and form various strands and meshes that are mostly composed of chitin (Williams & Cusack 2007). Chitin is also the main constituent of membranes (Williams & Cusack 2007). Modern lingulid (family Lingulidae) and discinid (family Discinidae) shells vary in the amount and composition of organic shell constituents, whereas discinids have an overall lower organic content than lingulids (Williams *et al.* 1998; Cusack & Williams 2007). The organic tissues of linguliform brachiopods have rather a directing role than a controlling function over shell apatite secretion (Neary *et al.* 2011).

Mineral constituents of the shell are different from the apatite mineral composing vertebrate bones and teeth (LeGeros *et al.* 1985; Rohanizadeh & LeGeros 2007). The apatite variety in modern linguliform shells has been inter-

puted on the basis of its IR and XRD characteristics and chemical composition as F-containing carbonate-OH apatite (LeGeros *et al.* 1985; Puura & Nemliher 2001). However, it is commonly referred to as francolite (an unofficial name for F-rich carbonated apatites), because the fluorine content in shell apatite can be as high as 3.5 wt% (Forchielli *et al.* 2014). The presence of OH⁻ anions in modern linguliform shell apatite has been suggested (LeGeros *et al.* 1985; Puura & Nemliher 2001; Rohanizadeh & LeGeros 2007). The infrared absorption bands indicative of the presence of OH⁻ anions have been described in the shells of modern *Lingula* heated in air (but not in N₂) to temperatures higher than 700 °C (Iijima *et al.* 1991). Shell apatite is reported to be crystalline (Schmahl *et al.* 2008) and crystallization is likely enhanced by shell proteins (Lévêque *et al.* 2004). However, in discinids the primary layer may also contain amorphous calcium phosphate (Merkel *et al.* 2007).

The composition of shell apatite somewhat varies in different brachiopod genera (LeGeros *et al.* 1985). The differences are perhaps best reflected in the carbonate ion content that is higher in *Glottidia* (3.6 wt%) than in *Lingula* (1.8–2.2 wt%) (Watabe & Pan 1984; LeGeros *et al.* 1985), whereas the average F content in highly calcified laminae in these genera is similar (2.5–2.6 wt%) (LeGeros *et al.* 1985). Variations in shell apatite chemistry have been recorded also inside the same shell. For example, LeGeros *et al.* (1985) noted that the F content is higher in exterior shell laminae and lower in interior ones. On the other hand, using microprobe analyses, Forchielli *et al.* (2014) showed, that the F content in the external shell layers of *Lingula anatina* is about 2.6 wt% and in the internal shell layer 3.5 wt%. They also report the variation in the Mg content in different shell laminae of *L. anatina* – 1.5 wt% in the external layer, 2.9 wt% in the median part of the shell and 2.4 wt% in the internal layer. Their EDS analyses further indicated that Na and S occur in the shell of *L. anatina* in trace amounts (Forchielli *et al.* 2014). Thermal decomposition experiments by Iijima *et al.* (1991) suggest that the shell apatite of *Lingula* may also contain some structural water. Chemical variations in apatite chemistry in the shells of the same species are probably also reflected in small variations in XRD lattice parameter values. For example, *a* varies between 9.386 and 9.396 Å and *c* between 6.859 and 6.864 Å for *L. anatina* (Puura & Nemliher 2001).

The shell apatite of living linguliforms is generally believed to be secreted in isotopic equilibrium with ambient sea water (Lécuyer *et al.* 1996), but this view has been argued by Rodland *et al.* (2003). In modern *Lingula* δ¹⁸O_{PO4} ranges within 19–23‰ (Lécuyer *et al.* 1998).

2.1.2. Nanostructures

Nanostructures have not been separately reported from modern linguliforms. However, the fibrillar shell organics as well as the apatitic aggregates in shells measure usually in nanoscale. The diameter of chitinous strands is ca. 30–60 nm (Williams *et al.* 1998) and of collagenous strands ca. 30–200 nm (Williams *et al.*

1994). The axial organic threads of bacula in *Glottidia pyramidata* are about 150 nm in diameter (Cusack *et al.* 1999 Plate 4 fig. 4). In discinids, these threads make up about one-third of the diameter of bacula (Williams *et al.* 1998).

The smallest mineral structures in linguliform brachiopod shells are spherical particles typically ca. 50 nm (sometimes up to 200 nm) in diameter (Williams *et al.* 1992, 1994, 1997, 1998; Williams & Cusack 1999; Schmahl *et al.* 2008), which in turn are composed of apatite granules 4–8 nm in diameter (Williams & Cusack 2007). All other higher-order apatitic structures in the shell are formed of such spherical particles. Most common apatite aggregates in shell structure made up of spherical particles are ellipsoidal particles, up to 1 μm long and 150 nm in diameter (Williams & Cusack 2007), but also other types of apatite aggregates are present that may differ between different brachiopod species. For example, typical apatitic bodies/aggregates in *Glottidia* are ovoids and ellipsoids, in the shell of *Lingula*, however, spheroidal (botryoids), ellipsoidal, but also fascicular apatitic bodies/aggregates can occur (Williams & Cusack 2007).

2.1.3. Microstructures

All brachiopod shells have laminated structure. Recent shells are composed of a rhythmic alternation of mineral-rich and organic-rich laminae. In the whole shell succession three main shell layers can be distinguished (Williams 1997): *periostracum* – the uppermost organic layer that is mostly not preserved in fossils, but may leave its imprints on the layer below it; *primary layer* – organic or mineralized layer below the periostracum, where the organic content may be high and the minerals may not be fully crystalline (Schmahl *et al.* 2008); and *secondary layer* – mineralized layer below the primary layer. Secondary layer defines shell structure and consists of alternating organic-rich and mineral-rich laminae.

The secondary layer comprises thinner laminae, of which the most universal (more or less similar in all living linguliforms) are compact laminae and membranous laminae. Compact laminae are composed of tightly arranged apatite aggregates and contain relatively few organics. The compact laminae in lingulids are in general a couple of micrometres thick, in discinids, however, about two times thicker (6–7 μm) (Williams *et al.* 1998). Membranous laminae are organic and very thin (a couple of hundred nanometres). In addition to compact and membranous laminae, also organic-rich structural laminae exist (e.g. baculate, botryoidal, virgose, rubbly and stratified laminae; Williams & Cusack 1999), the most characteristic/dominant of which gives the name to shell structure. Modern lingulids have two main shell structure types: botryoidal/virgose (*Lingula*) and baculate (*Glottidia* and discinids) (Table 1).

The shells of modern discinids and the species belonging to the lingulid genus *Glottidia* have baculate structure (Table 1) (Iwata 1982; Williams *et al.* 1992, 1998; Cusack *et al.* 1999; Williams & Cusack 1999; Merkel *et al.* 2007; Schmahl *et al.* 2008). They differ structurally from the shells of another

common living lingulid *Lingula* that has virgose (botryoidal) shell structure (Williams *et al.* 1994; Cusack *et al.* 1999; Williams & Cusack 1999, 2007). Baculate shell structure is characterized by the alternation of compact and partly mineralized baculate laminae with apatitic rods (called bacula) that form a criss-cross (trellised) pattern alternating with other structural laminae. The outermost secondary layer is composed of stratified laminae that grade inwardly into a baculate zone (Williams *et al.* 1992; Cusack *et al.* 1999; Williams & Cusack 1999). The inner part of the shell (inner or internal zone that can be up to 100 μm thick in discinids) is composed of a condensed succession of compact laminae alternating with thin intercalations of a high organic content (Iwata 1982; Williams *et al.* 1992; Williams & Cusack 2007). Baculate sets are asymmetrical and grade from a biomineral-rich compact lamina inwardly into a baculate lamina and terminate in a membranous lamina in *Glottidia* (Cusack *et al.* 1999), however, in *Discina* the rhythm is reverse, from predominantly organic to mainly apatitic laminae (Williams *et al.* 1992). The thickness of individual bacula is varying, but is typically less than 1 μm (ca. 750 nm in *G. pyramidata*, ca. 400 nm in *G. palmeri*, 150–250 nm in *Discinisca*) (Williams *et al.* 1998; Cusack *et al.* 1999; Williams & Cusack 1999, 2007). In discinids in general, bacula are very fine, 70–350 nm in thickness (Williams *et al.* 1992, 1998; Williams & Cusack 1999; Merkel *et al.* 2007; Schmahl *et al.* 2008). Bacula are made of linearly organized apatitic ovoids, cylindroids or individual spherical particles that are aggregated around axial, probably proteinaceous strands (Williams & Cusack 1999). However, some bacula are composed of pinacoidal plates orthogonally aligned by epitaxy or screw dislocation (Cusack *et al.* 1999; Williams & Cusack 1999). The configuration of bacula can be very variable: inside the same shell the bacula can be built up of gently flexured vertical rods or criss-crossed rods inclined about 60° to the bounding surfaces, or have almost horizontal position (Williams & Cusack 1999).

In addition to baculate laminae, other structural laminae occur in the same shells, for example rubbly or virgose laminae where baculation is not well developed, but which are composed of various aggregates made of spherical apatite particles enmeshed into largely fibrillar organics (Williams & Cusack 1999). Also, individual spherical apatite particles may cover the chitino-proteinaceous mats as well as strands and meshes supporting bacula (Cusack *et al.* 1999; Williams & Cusack 1999). It has been noted that geographical and environmental factors do not affect much the shell structure and composition of living linguliforms, but shells of different genera and different species have a different number of mineralized laminae (Forchielli *et al.* 2014).

2.2. Fossil linguliforms

2.2.1. Shell composition

The XRD analyses of fossil linguliform shells suggest rapid post-mortem alteration of shell apatite (Puura & Nemliher 2001), which results in the lowering of the lattice parameter values (Nemliher *et al.* 2004). The analyses also show that there may be two coexisting apatite phases in at least some fossil shells. One of the apatite phases has the lattice parameter values similar to apatite in modern linguliforms, the other phase is suggested to be diagenetic (Nemliher *et al.* 2004). Fossil shell apatites are also enriched in rare earth elements (REE) (Lécuyer *et al.* 1998) and phosphate $\delta^{18}\text{O}_{\text{PO}_4}$ values in linguliform brachiopods are typically about 15–16‰, at least in Tremadocian obolids (Lécuyer *et al.* 1998).

2.2.2. Nanostructures

Nanostructures have not been separately reported from fossil linguliforms. Occasionally, however, organic constituents of fossil shells have not been completely degraded during fossilization (Cusack & Williams 1996; Williams & Cusack 1997; Williams *et al.* 1998). Phosphatized threads reminiscent of the nets of collagen or actin have been described from Carboniferous *Lingula* (Cusack & Williams 1996). The mineral aggregates of the shell may also be preserved in nanometric fidelity and the recrystallization of shell apatite is suggested to be pseudomorphous (Cusack & Williams 1996; Williams & Cusack 1997; Williams *et al.* 1998).

2.2.3. (Baculate) microstructures

The shell structure of fossil linguliforms is believed to be capable of preserving in nanometric detail. Even if it is fully recrystallized into prismatic apatite crystallites of different size, it is usually possible to make conclusions about the original shell structure (Cusack & Williams 1996). Baculate sets are somewhat different in fossil linguliforms, being subtended between two compact laminae (baculate symmetrical shell structure) instead of being placed between a compact and a membranous lamina (baculate asymmetrical shell structure) as in modern linguliforms (Williams & Cusack 1999). Baculate structures appear to be more variable in fossil linguliforms and some species, for example species belonging to the genus *Eoobolus*, may have different shell structures (Streng *et al.* 2008). Another type of baculate shell structures has also been defined – orthogonal baculate structure (also called non-penetrative columnar structure, Holmer *et al.* 2008) that resembles a columnar structure but columns are thinner than typical acrotretide-type columns, lack central axial canals and compact laminae remain imperforated (Holmer *et al.* 2008; Streng *et al.* 2008). This type of shell structure has been observed in *Curticia? pattersonensis* from the upper Series 3 of the Cambrian (*Cedaria–Crepicephalus* zone) of the Great Basin, USA (Streng & Holmer 2005; Streng *et al.* 2008), acrothelid brachiopod

Eothele tubulus from Cambrian Series 2, Stage 4 of Thomasville, Pennsylvania (Skovsted & Peel 2010), *Aboriginella* (former 'Upper Cambrian', Kazakhstan; Holmer *et al.* 2008), *Vaculina* (former 'Middle Cambrian', *Glyptagnostus stolidotus* Biozone, Kazakhstan; Holmer *et al.* 2008) and possibly in *Dysoristus* (former 'Upper Cambrian', Kazakhstan; Cusack *et al.* 1999; Holmer *et al.* 2008). *Eothele tubulus* is described as the oldest brachiopod with baculate shell structure known by now, whereas orthogonal and inclined bacula co-occur in the shells of this species (Skovsted & Peel 2010).

3. MATERIAL

This thesis is based on four detailed studies of the shells of **1)** *Obolus ruchini* Khazanovitch *et* Popov (Paper II) collected from the locality at the Volkhov River (Russia), from the Sablinka Formation (Gertovo Member) of Cambrian Series 3 (former 'Middle Cambrian'); **2)** *Ungula inornata* (Mickwitz) (Paper III) collected from the Ülgase outcrop (Estonia), Ülgase Formation, Furongian; **3)** *Ungula ingrlica* (Eichwald) (Paper IV) collected from the Iru and Ülgase outcrops (Estonia) below the lower boundary of the Ordovician System, in the Kallavere Formation (Maardu Member) and **4)** *Bicarinatina bicarinata* (Kutorga) (Paper I) collected from the Poruni River and Gorodenka Stream and dated as the Middle Devonian (Narva Age). All the shells originate from poorly lithified argillaceous sandstones. Most of the selected species (except *B. bicarinata*) belong to the family Obolidae that serves for typification of the baculate shell structure in fossil linguloids (Cusack *et al.* 1999).

The valves of *U. ingrlica* from the uppermost Furongian were subjected to chemical analyses, because distinct apatite phases were previously suggested to exist in the valves of this species (Nemliher 1999 fig. 8; Puura & Nemliher 2001). The valves were chosen from different stratigraphic levels in the Furongian (the upper and lower coquinas at Iru and Ülgase) according to their completeness and colour. Lighter (brown) valves were preferred to avoid heavily pyritized specimens. The results of chemical analyses were compared with the data from modern *Lingula anatina* originating from Cebu Island, the Philippines.

4. METHODS

Methods for shell structure studies were chosen to be as little destructive as possible. The valves were hand-picked from loose, poorly cemented sandstones, manually cleaned under a binocular microscope if necessary and broken along their medial axis to expose all the shell laminae (Fig. 1). Fresh fracture surfaces were mounted on SEM stubs using a conductive tape. Such a sample treatment was used to avoid possible destruction of fragile structures or loss of information due to polishing, etching or any other chemical treatment.

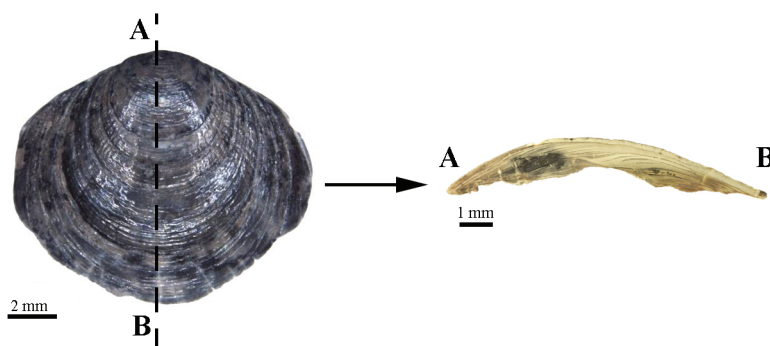


Figure 1. Brachiopod (*Ungula ingrca*) valve broken along its medial axis to expose the shell laminae.

Most of the shell structure studies reported in Papers I–IV were carried out on untreated and uncoated fracture surfaces using SEM in variable pressure mode and images were collected with a backscattered electron (BSE) detector. Leo1450VP SEM at the Geological Survey of Norway (Papers I, II) and Zeiss EVO MA15 SEM at the University of Tartu, Department of Geology (Papers III, IV) were employed. In the SEM-BSE regime, the beam of primary electrons interacts with the sample surface where electrons change their trajectories due to elastic scattering that is controlled by the average atomic number of elements in the sample. The SEM-BSE images bear compositional information of the sample, but also highlight shell structural details (Balthasar *et al.* 2009).

To understand the difference between the images created using backscattered and secondary electron (SE) detectors, both of these regimes were used in Paper III. Secondary electrons are inelastically ejected from the specimen surface and are used to describe the topography of the specimen. To study apatite crystallite morphology at high magnifications (Paper IV), the fracture surface of *Ungula ingrca* was coated with a ca. 5 nm thick Pt layer and was studied in high vacuum mode.

X-ray diffraction analyses were carried out on the valves of *U. ingrca* to study the structural characteristics of apatite phases. For this purpose individual valves were hand-ground in an agate mortar, and XRD preparations were made on zero-background silicon mono-crystal sample holders for mineral analysis.

The XRD patterns were collected with a Bruker D8 Advance diffractometer with $\text{CuK}\alpha$ radiation using a LynxEye linear detector. The mineral composition and structure refinement of apatite phases was modelled using Topas 4 code.

The varieties of apatite (general formula $\text{Ca}_5(\text{PO}_4)_3(\text{F},\text{OH},\text{Cl})$) can be differentiated, in addition to their unit cell dimensions, also by elemental and anionic composition. To study the spatial variability of apatite chemistry in *U. ingrica* valves, the Thermo Scientific Nicolet iN10 MX Fourier transform infrared (FTIR) microscope in Attenuated Total Reflectance (ATR) mode and analytical SEM (EDS) were used, both in the mapping regime. Attenuated total reflectance mapping was performed using a slide-on ATR objective with a conical germanium crystal, in the wavenumber range $4000\text{--}550\text{ cm}^{-1}$, at a spectral resolution of 4 cm^{-1} . Spectral maps were further processed by means of OMNIC PICTA software. Elemental analysis (EDS mapping) was performed on SEM equipped with the Oxford X-MAX 80 energy dispersive detector system and Aztec Energy software. The combination of these methods covers all principal compositional variabilities of apatite. The elemental and anionic composition of apatite is varying due to a multitude of chemical substitutions possible in the apatite crystal structure (Hughes & Rakovan 2002). For example, calcium can be substituted by other cations (e.g. Na^+ or Mg^{2+}), phosphate (PO_4^{3-}) anions are most commonly substituted by carbonate (CO_3^{2-}) anions; OH^- and F^- occur in structural channel sites in the apatite crystal lattice and most commonly substitute each other or are substituted by Cl^- (Pan & Fleet 2002). Carbonate anions in the apatite crystal lattice can further be located either in the structural channel along the crystallographic *c*-axis (referred to as A-type carbonate) or as a substituent for phosphate anions (B-type carbonate) (Elliott 2002). Using SEM-EDS analysis, we can study the variations in the elemental composition of apatite (Na, Mg and other cations that could possibly substitute for Ca, and also F or Cl). The FTIR technology is based on the vibrations of certain bonds in molecules or ions when irritated with infrared light. In apatites it is used to study mainly the occurrence and nature of the P–O (PO_4^{3-}), C–O (CO_3^{2-}) and O–H (OH^- , H_2O) bonds (e.g. Elliott 2002; Antonakos *et al.* 2007). Recently ATR mapping using FTIR microscopy was also adopted for spatial study of diagenesis in bones (e.g. Reiche *et al.* 2010; Lebon *et al.* 2011) and for characterizing the composition and structure of phosphatized and/or organic microfossils (Igisu *et al.* 2014).

The valves of *U. ingrica* are quite big (thickness up to around 1 mm) and the compact laminae in these valves may occasionally be much thicker than typical $2\text{ }\mu\text{m}$ in many other linguliforms. As these valves are still composed of two apatite phases, they are well suited for ATR-FTIR and SEM-EDS analyses. For the analyses, the valves were embedded in plastic resin and ground with silicon carbide paper in successive finer steps and finally polished with diamond paste of $1\text{ }\mu\text{m}$ grain size until the medial cross sections of valves were exposed (Fig. 1). For compositional SEM-EDS analyses, the polished sample surface was coated with a 3–5 nm thick layer of carbon.

5. RESULTS

5.1. Baculate shell structure (Papers I–IV)

5.1.1. General notes on preservation

Structural details of the studied valves are illustrated in Figures 2–4. All the studied shells were collected from sandstones and exhibit variable preservation (Fig. 2). The preservation state of the recognizable shell structures varies in different shells from the same locality, as well as in shells of the same species from different localities (Figs 2–3). This indicates that each individual valve characterizes its own post-mortem diagenetic traits. Consequently, some valves exhibit shell structures better than the others and some valves are so heavily recrystallized that shell structures cannot be revealed (e.g. *Ungula ingraca* in Fig. 2; Fig. 3G). The preservation of shell structures may also vary within the same valve. Although several valves of each species were studied, only a few showed structural peculiarities well enough to be selected for detailed description. However, the studied valves of Cambrian Series 3, Furongian and Devonian linguliforms revealed similar preservational trends.

The shells are typically composed of alternating compact and baculate laminae, with external (older) baculate laminae being thicker ($>100\ \mu\text{m}$) than internal (younger) ones (about $2\text{--}10\ \mu\text{m}$) (Fig. 2). External baculate laminae tend to be more densely filled with apatite (Fig. 2) and contain thicker (up to $3\ \mu\text{m}$ in diameter) bacula (Fig. 3) that may also be fused together due to up to the several micrometres long apatite fascicles and dumbbells that usually grow radially from the axis of bacula (Fig. 3A, C, E). Mineralized bacula become (gradually) thinner towards the interior side of the valves (Figs 2–4). For example, in *Ungula inornata* (Paper III) the bacula in the outermost baculate laminae are up to $3\ \mu\text{m}$ in diameter, whereas the bacula in the central baculate laminae are about $1\ \mu\text{m}$ thick. The thickness of bacula in *Bicarinatina bicarinata* (Paper I) is varying as well, ranging from 0.25 to $0.5\ \mu\text{m}$.

The inclination of bacula is also varying throughout the valves. In many baculate laminae the bacula are oriented at right angle to their bounding surfaces (Fig. 2 *Obolus ruchini*, *B. bicarinata*; Fig. 3C–F). Laminae, representing the typical inclined bacula forming a trellised (criss-cross) structure as described in Holmer (1989), are rather rare (Fig. 2 *U. inornata*; Fig. 3C).

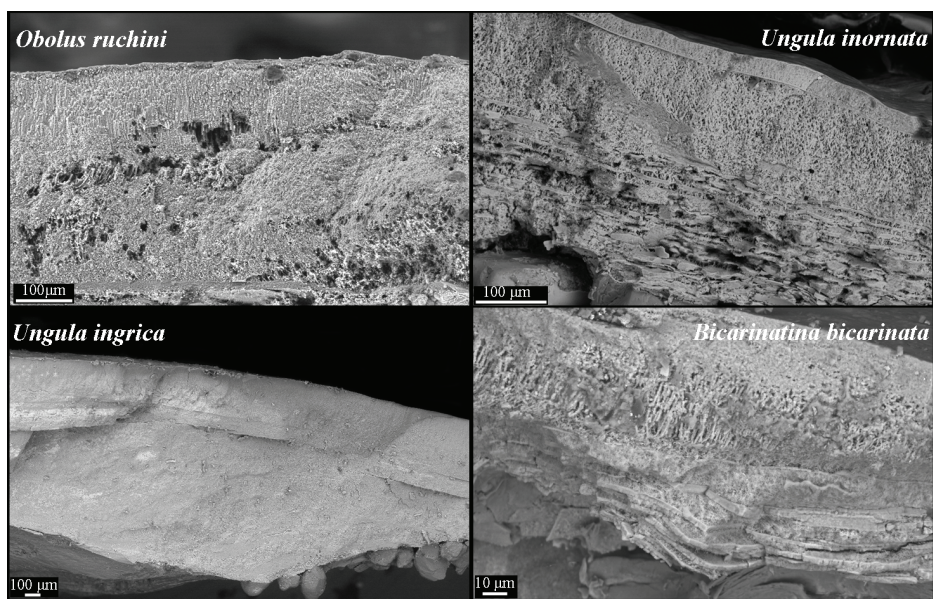


Figure 2. Different preservation state of baculate structures in a single valve. In all the studied valves bacula are thicker and commonly fused in the external part of the valve. *Obolus ruchini* (TUG 1386-1; supplementary (unpublished) image related to Paper II) – bacula are thicker in the external part of the valve and thinner in the central and internal parts of the shell; nanofibrils are located in the ‘holes’ in the central and internal parts of the valve. *Ungula inornata* (TUG 1323-4; supplementary (unpublished) image related to Paper III) – thick baculate lamina in the external part of the valve contains thick bacula that are commonly fused together; baculate laminae in the central part of the valve contain thinner bacula; some of the laminae in the internal part of the valve show nanofibrils. *Ungula ingraca* (TUG 1232-7; supplementary (unpublished) image related to Paper IV) – valves are composed of dense apatite aggregates; thick remains of bacula are found only in the innermost lamina. *Bicarinatina bicarinata* (TUG 1323-1; Paper I Fig. 3B) – bacula are fused together in the exterior baculate laminae, whereas in central baculate laminae bacula are preserved; internally positioned baculate laminae show well-preserved thin nanofibrils.

Apatite in shells occurs commonly as needle- (in SEM-BSE images; Fig. 3A, E, G) or lath-like (in SEM-SE images; Fig. 3H) prismatic crystallites that may form fascicle-, dumbbell-shaped or spherulitic aggregates. Also, the homogeneous mass (cryptocrystalline calcium phosphate, Holmer 1989) filling the baculate laminae of *U. ingraca* is composed of very small lath-like apatite crystallites (Fig. 3H). Prismatic crystallites associated with bacula usually project from the axis of the bacula (Fig. 3A, C–F). Prismatic crystallites associated with compact laminae also project from the laminae (Fig. 3G). Compact laminae may alternatively be composed of small (ca. 50 nm in diameter) sub-hedral spherical crystallites (Fig. 3H).

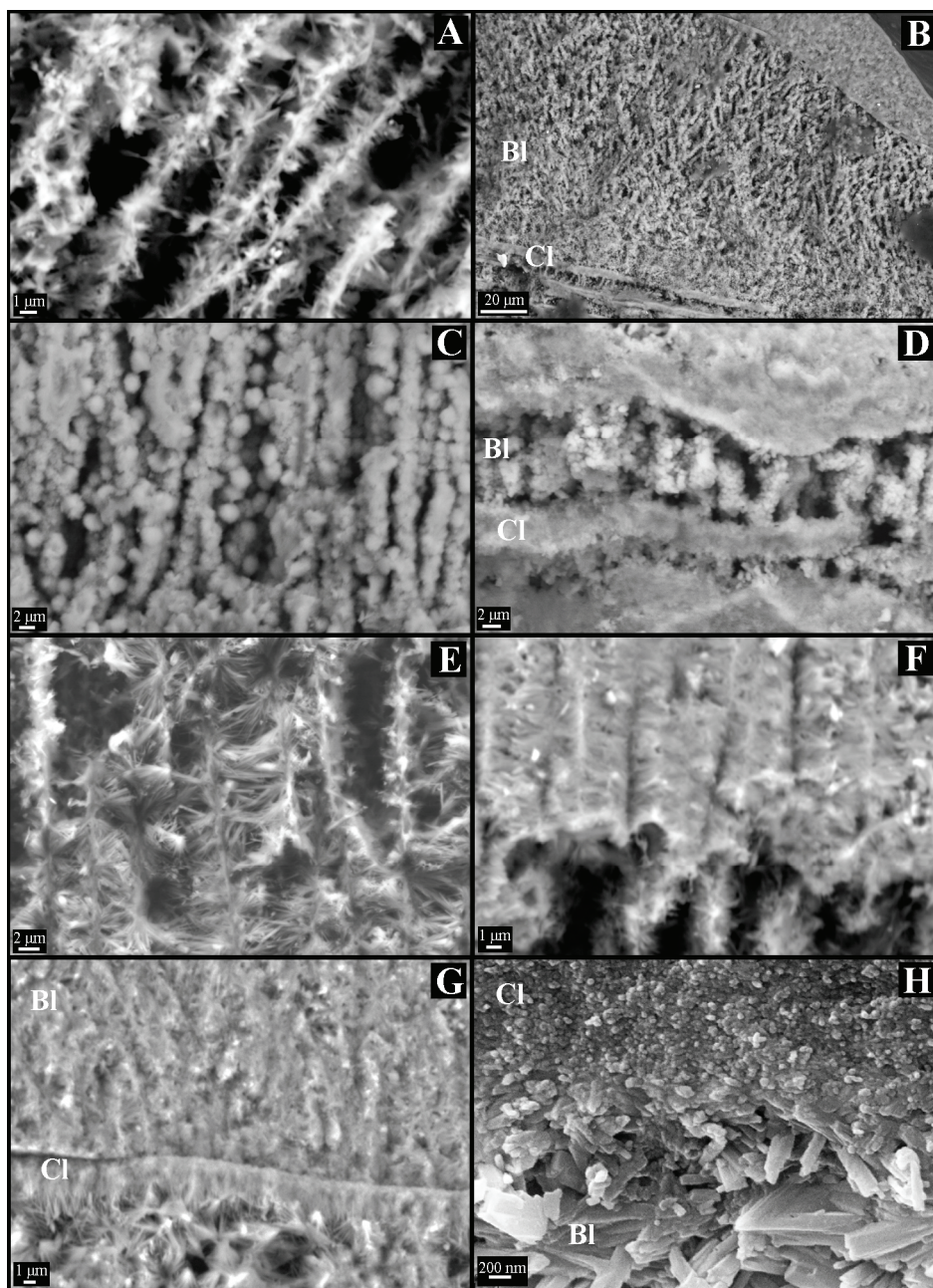


Figure 3. SEM-BSE close-ups of bacula from the valves of *Obolus ruchini* TUG 1386-1, Paper II (A, E–G), *Ungula inornata* TUG 1323-4, Paper III (B, C) and *Ungula ingrca* TUG 1323-7 (D) and TUG 1323-9 (H), Paper IV. A: thin bacula covered with prismatic apatite crystallites (supplementary (unpublished) image related to Paper II). B: thick baculate lamina close to the external shell surface showing thick bacula with criss-cross arrangement (Paper III Fig. 3D). C: bacula covered with spherulitic apatite aggregates (Paper III Fig. 3G). D: thick column-like bacula (supplementary (unpublished) image related to Paper IV). E: bacula starting to fuse

together due to large prismatic crystallites covering them (supplementary (unpublished) image related to Paper II). F: bacula fused together (supplementary (unpublished) image related to Paper II). G: baculate lamina with fused bacula and a compact lamina replaced by prismatic crystallites and aggregates (supplementary (unpublished) image related to Paper II). H: SEM-SE image of the transition between a compact lamina and a baculate lamina in *Ungula ingraca*; the compact lamina is composed of spherical subhedral apatite crystallites of about 50 nm in diameter, whereas the baculate lamina is composed of larger prismatic lath-like crystallites (Paper IV Fig. 7). BI – baculate lamina; CI – compact lamina.

5.1.2. Nanofibrils

Narrow fibrils, thinner than bacula (here called nanofibrils), were found in the valves of *O. ruchini* (Paper II), *U. inornata* (Paper III) and *B. bicarinata* (Papers I, II). Nanofibrils are usually found in baculate laminae closer to interior sides of the brachiopod valves (Fig. 2 *U. inornata*, *B. bicarinata*) but can also be found in occasional ‘windows’ in the central parts of the cross section of *O. ruchini* (Fig. 2 *O. ruchini*). The SEM-BSE and SE studies (Paper III) have revealed that nanofibrils have very small diameters (about 100–200 nm) (Fig. 4). Some of the nanofibrils are distinctly curved (Fig. 4A, D). In some areas of the shell the fibrils have a tightly reticulate appearance (Fig. 4D). The fibrils are only occasionally covered with rare larger apatitic crystals (Fig. 4A, C).

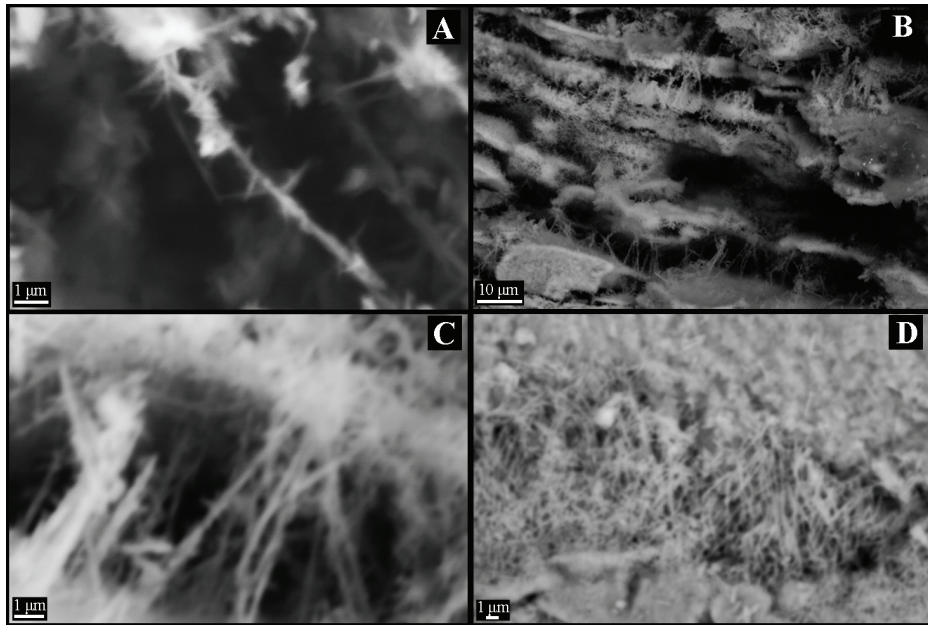


Figure 4: SEM-BSE images of nanofibrils in the shells of *Obolus ruchini* (A; TUG 1386-1, Paper II Fig. 3G), *Ungula inornata* (B, C; TUG 1323-4, Paper III Fig. 3E, F) and *Bicarinatina bicarinata* (D; TUG 1323-1, Paper I Fig. 3F).

5.2. Chemical composition of valve apatite (Paper IV)

ATR-FTIR and SEM-EDS mapping indicates that at least two different apatite phases are present in the shells of Cambrian *Ungula ingraca*. The distribution of phases in a shell tracks the distribution of compact and baculate laminae (Fig. 5A–C) and it is possible to characterize the chemical and structural differences of apatite in compact and baculate laminae (Table 2).

Table 2. Main differences between the apatite phases in compact and baculate laminae according to the ATR-FTIR and SEM-EDS analyses.

	Apatite in compact laminae	Apatite in baculate laminae
Carbonate IR bands	Weaker	Stronger
Dominant ν_2 CO_3^{2-} band	872 cm^{-1}	864 cm^{-1}
Relative amount of F	Less	More
Relative amount of Ca	Less	More
Relative amount of Na and Mg	(Slightly) more	(Slightly) less
Crystallite size and morphology	Spherical particles with diameter of about 50 nm	Prismatic crystallites, >1 μm in length, can form fascicular or dumbbell-shaped aggregates

Apatite in compact laminae is characterized by the ATR bands (Fig. 6) (interpreted after LeGeros *et al.* 1985; Dahm & Risnes 1999; Elliott 2002; Rodríguez-Lorenzo *et al.* 2003; Antonakos *et al.* 2007; Rintoul *et al.* 2007; Rohanizadeh & LeGeros 2007; Fleet & Liu 2008; Stathopoulou *et al.* 2008; A and B refer to the type of carbonate substitution) at the following wavenumbers:

- $\sim 3535 \text{ cm}^{-1}$ – a very weak IR band (seen only in magnified spectra) that is formed due to O–H stretching vibrations in OH^- anion
- $\sim 3400 \text{ cm}^{-1}$ – a weak broadband centred at about 3400 cm^{-1} that is formed due to O–H stretching vibrations in molecular water (H_2O)
- $\sim 1630 \text{ cm}^{-1}$ – a weak broadband centred at about 1630 cm^{-1} that can be assigned to O–H bending vibrations in the molecular water (H_2O)
- $\sim 1455 \text{ cm}^{-1}$ – IR band formed due to C–O asymmetric stretching vibration (ν_3) in CO_3^{2-} anion (B), occurs as a doublet band with the band at $\sim 1425 \text{ cm}^{-1}$
- $\sim 1425 \text{ cm}^{-1}$ – IR band formed due to C–O asymmetric stretching vibration (ν_3) in CO_3^{2-} anion (B), occurs as a doublet band with the band at $\sim 1455 \text{ cm}^{-1}$

- ~1090 cm^{-1} – IR band formed due to P–O stretching vibrations in the PO_4^{2-} anion (ν_3)
- ~1018 cm^{-1} – the most intensive IR band in apatite spectra, is formed due to P–O stretching vibrations in the PO_4^{2-} anion (ν_3)
- ~964 cm^{-1} – also a very intensive IR band, formed due to P–O stretching (ν_1) vibrations in the PO_4^{2-} anion
- ~880 cm^{-1} – very weak shoulder due to C–O out-of-plane bending (ν_2) in the CO_3^{2-} anion (A)
- ~872 cm^{-1} – weak band formed due to C–O out-of-plane bending (ν_2) in the CO_3^{2-} anion (B)
- ~866 cm^{-1} – weak band formed due to C–O out-of-plane bending (ν_2) in the CO_3^{2-} anion (B)
- ~749 cm^{-1} – very weak band formed due to O–H librational vibration in the OH^- anion

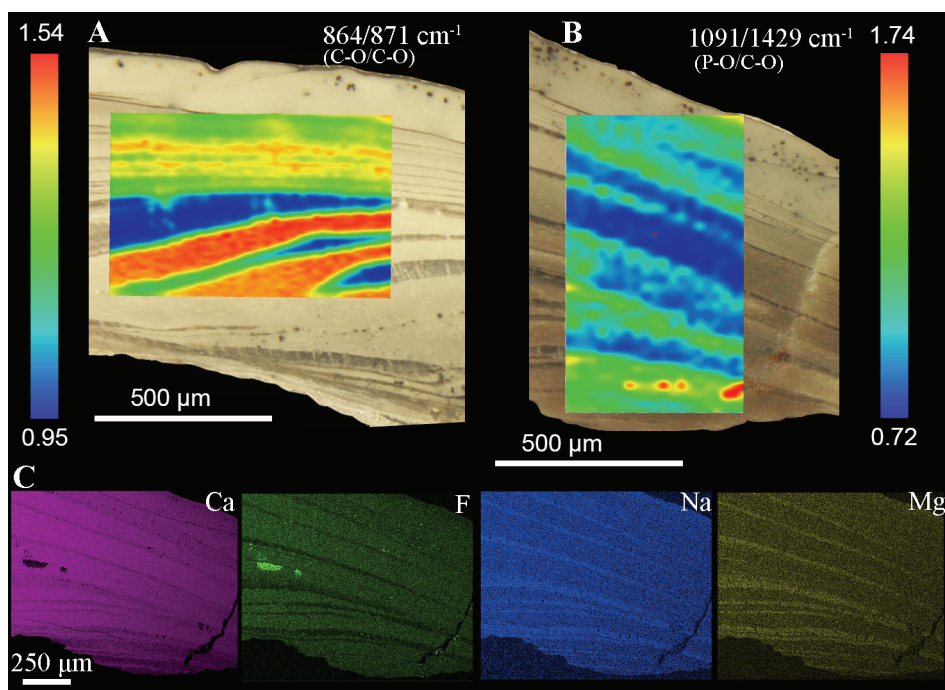


Figure 5. Variability of apatite composition in a valve of *Ungula ingraca* (TUG 1323-6, Paper IV) in ATR (A, B) and EDS (C) maps. (A) ATR map showing 864 cm^{-1} /871 cm^{-1} band ratio variation – there is more diagenetic carbonate (wavenumber 864 cm^{-1}) in apatite in baculate laminae and less in compact laminae (Paper IV Fig. 6C). (B) ATR map showing 1091 cm^{-1} /1429 cm^{-1} band ratio variation – compact laminae are richer in phosphate than baculate laminae where carbonate anions (indicated by a band at 1429 cm^{-1}) are more common (Paper IV Fig. 6B). (C) SEM-EDS maps of Ca, F, Na and Mg show that compact laminae contain less Ca and F (darker thin bands in Ca and F images) and more Na and Mg (lighter thin bands in Na and Mg images) compared to baculate laminae (thicker bands) (Paper IV Fig. 4).

These bands indicate that apatite in compact laminae has PO_4^{2-} and CO_3^{2-} anions in its crystal lattice, possibly also small amounts of OH^- . B-type carbonate substitution prevails, however, small amounts of A-type carbonate may also be present. Molecular water may occur either on the sample surface or in the apatite crystal lattice.

Based on SEM-EDS (Fig. 5C) mapping, apatite in compact laminae has less Ca, which is partly substituted by Na and Mg, and also less F than apatite in baculate laminae.

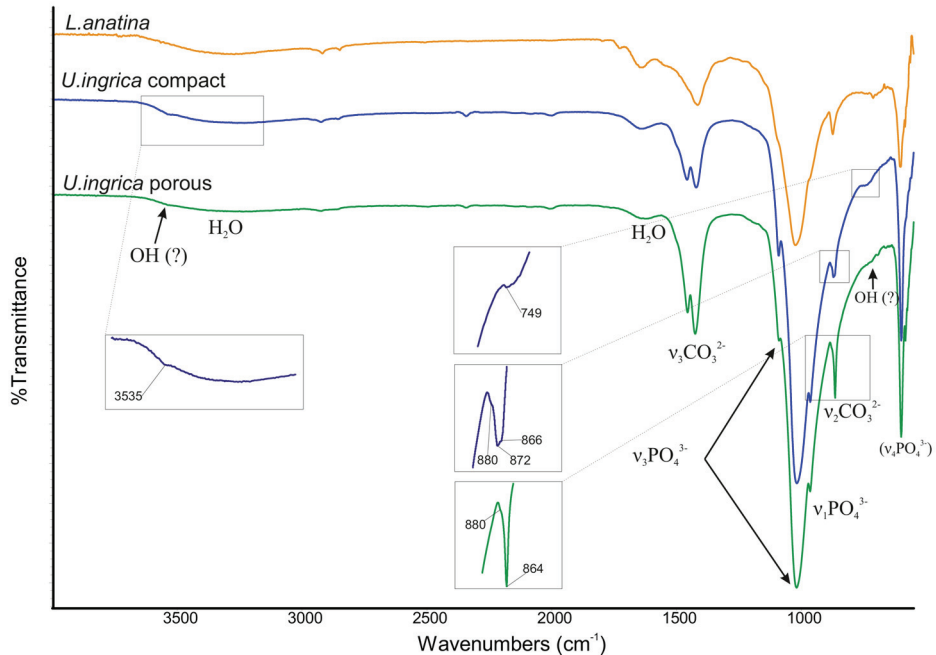


Figure 6. ATR spectra from the compact (blue line) and baculate (green line) laminae of *Ungula ingrica* (TUG 1323-6) compared to an ATR spectrum of shell apatite of modern *Lingula anatina* (GIT 587-32) from the Philippines (yellow line) (Paper IV Fig. 5).

Apatite in baculate laminae is somewhat different from apatite in compact laminae. The phase in baculate laminae has essentially the same ATR bands as the phase in compact laminae (Fig. 6). However, the difference appears in the $\nu_2 \text{CO}_3^{2-}$ region, where a diagnostic strong band at 864 cm^{-1} replaces the 872 cm^{-1} band that is characteristic of compact laminae (Figs 5A, 6). Also, the intensity of all C–O vibration bands is higher in baculate laminae (Fig. 6), indicating that this apatite has more carbonate ions in its crystal lattice. According to SEM-EDS mapping (Fig. 5C), the apatite in baculate laminae has more Ca, less Na and Mg and more F than the apatite in compact laminae.

The elemental (Ca, Mg, Na) differences between the apatite phases in compact and baculate laminae, however, are only minor according to EDS point measurements. Both apatite phases contain more Na than Mg but the differences between the phases are small as the content of either of the elements is less than 1 wt%. The greatest differences are observed in the F content, which is about 2–3 wt% in compact laminae, but often higher than 3.7 wt% in baculate laminae. These results, however, should be treated with caution, because the characteristic X-rays generated from light elements (including fluorine) are difficult to measure and quantify with EDS.

Two different apatite phases in the studied valves of *U. ingrica* are further confirmed by XRD analyses that show discrete phases differing mostly in *a*-axis values (Table 3). One of the phases has the refined lattice parameter values $a = 9.340 - 9.347 \text{ \AA}$ and $c = 6.896 - 6.899 \text{ \AA}$; in the other one $a = 9.377 - 9.397 \text{ \AA}$ and $c = 6.891 - 6.896 \text{ \AA}$.

Table 3. Refined lattice parameter values for two apatite phases (Apatite 1 and Apatite 2) in the valves of *U. ingrica* (TUG 1323-5) from two levels in the Iru outcrop (I5 and I7/Iru7) and from the Ülgase outcrop (Ü); Paper IV.

Sample	Apatite 1 (Å)		Apatite 2 (Å)	
	<i>a</i>	<i>c</i>	<i>a</i>	<i>c</i>
I-I5-d	9.346	6.896	9.391	6.891
I-I5-v2	9.344	6.897	9.394	6.894
I-I5-v	9.342	6.899	9.377	6.896
Iru7	9.344	6.897	9.389	6.893
I-I7-v2	9.340	6.898	9.397	6.894
I-I7-v3	9.346	6.898	9.391	6.895
I-I7-v	9.342	6.899	9.394	6.894
I-Ü-3-d	9.347	6.897	9.383	6.893
I-Ü-3-v2	9.344	6.899	9.388	6.893
I-Ü-3-v	9.344	6.899	9.386	6.892

6. DISCUSSION

6.1. Shell apatite phases and their origin (Paper IV)

Nemliher *et al.* (2004) have shown the existence of two apatite phases in the shells of Cambrian *Obolus apollinis*. However, the method used in earlier research did not allow the authors to locate the discovered apatite phases and fossil linguliform shells are therefore interpreted as being composed of a mixture of several apatite phases (Puura & Nemliher 2001; Nemliher *et al.* 2004; Cusack & Williams 2007). The XRD analyses of the valves of *Ungula ingrlica* made in this study confirmed the existence of two apatite phases in these linguliforms; the adjusted lattice parameters are: $a = 9.340 - 9.347 \text{ \AA}$, $c = 6.896 - 6.899 \text{ \AA}$ for phase 1 (Apatite 1) and $a = 9.377 - 9.397 \text{ \AA}$, $c = 6.891 - 6.896 \text{ \AA}$ for phase 2 (Apatite 2) (Table 3). These results are well comparable with the lattice parameter values obtained by Nemliher *et al.* (2004). During their experiment valves of Furongian *O. apollinis* were heated to different temperatures until 1000 °C and they concluded that one of the apatite phases had the lattice parameter a values higher than 9.37 Å, whereas the other, likely diagenetically changed apatite phase had the lattice parameter a values below 9.37 Å.

The distribution of these apatite phases was established in this study using ATR and EDS mapping (Fig. 5). The results show that in case of *U. ingrlica* valves the different apatite phases follow the structural laminae of the shell. Compact laminae and baculate laminae have different chemical compositions (Table 2). The differences are best expressed in the lower CO_3^{2-} and F content and in higher compositional variation in the cationic positions in apatite in compact laminae in comparison with the apatite phase in baculate laminae. Apatite unit cell dimensions along the a -axis are considered to diminish with increasing amounts of CO_3^{2-} anions substituting for the PO_4^{2-} anion and with F^- anions substituting OH^- in apatite structural channel sites (Elliott 2002; Yao *et al.* 2009). Considering this fact, it is evident that the phase with lower lattice parameter a values (Apatite 1) represents the phase in baculate laminae, and the phase with higher lattice parameter a values (Apatite 2) is the one found in compact laminae. On the other hand, also the occurrence of OH^- or CO_3^{2-} (A-type carbonate substitution) in the apatite structural channel sites could rise the lattice parameter values. According to FTIR data, some of the A-type carbonate substitution may be present in both apatite phases (indicated by the weak shoulder at the wavenumber about 880 cm^{-1} in fossil brachiopod apatite spectra (Fig. 6; Paper IV). The presence of OH^- in the linguliform shell apatite has been suggested for both modern (LeGeros *et al.* 1985; Puura & Nemliher 2001; Rohanizadeh & LeGeros 2007) and fossil (Veiderma & Knoubovets 1972; Iijima *et al.* 1991; Nemliher *et al.* 2004) taxa. The IR spectra of *U. ingrlica* (Fig. 6) also hint at the presence of O–H bands in shell apatite, however, their intensity is very weak and does not give any spatial variation in ATR maps.

Furthermore, the appearance of O–H bands at about 3535 and 749 cm^{-1} has been suggested to indicate a high F^- content, at least in calcined phosphate spectra (Rodríguez-Lorenzo *et al.* 2003). Therefore, OH^- substitution in the apatite structural channels cannot explain the shift in unit cell parameters and the greatest effect on the XRD lattice parameters in the studied shells is most likely due to differences in CO_3^{2-} and F^- contents. These results agree with the interpretation by Nemliher *et al.* (2004) that higher XRD lattice parameter values could be associated with the phase in compact laminae.

Compact laminae are thought to be the best preserved parts of fossil linguliforms (e.g. Cusack & Williams 1996). This assumption, however, is not proven chemically, but is based on morphological similarities in apatite crystal shape and size between fossil and modern linguliforms. Indeed, the compact laminae in *U. ingrlica* are composed of apatite crystallites similar in size to spherical apatite particles in modern brachiopods (Williams & Cusack 2007; Schmahl *et al.* 2008). Apatite crystallites in baculate laminae, on the other hand, are larger and prismatic in shape, and this is indicative of diagenetic recrystallization. When comparing the apatite composition in compact laminae in Furongian *U. ingrlica* with the composition known in modern linguliforms, several similarities, but also some differences can be seen. Nemliher *et al.* (2004), for example, have noticed similarities between XRD lattice parameter *a* values in one of the apatite phase from fossil *Obolus* with the apatite phase in modern *Lingula*. The same result was obtained also in this study, showing that the lattice parameter *a* values of Apatite 2 in *U. ingrlica* are very similar to the ones in modern *Lingula* as well as the ones in modern *Glottidia* (Fig. 7).

The FTIR studies further confirm that the CO_3^{2-} content in compact laminae of *U. ingrlica* is roughly similar to the CO_3^{2-} content in modern linguliforms. This can be evaluated by comparing the intensities of IR bands resulting from the vibrations in carbonate anions between the spectrum from the compact lamina of *Ungula* and the spectrum of modern *Lingula* (Fig. 6). Energy dispersive spectroscopy also shows that apatite in compact laminae contains less fluorine and its content (about 2–3 wt%) is rather similar to the one measured from modern lingulids (1.6–3.5 wt%, LeGeros *et al.* 1985; Aoba *et al.* 2003; Forchielli *et al.* 2014). Furthermore, a specific IR band at the wavenumber 872 cm^{-1} characterizes the apatite phase in compact laminae of *Ungula*. A carbonate IR band at this position is characteristic of biological apatites (Elliott 2002), including shell apatite of modern *Lingula* (LeGeros *et al.* 1985; Rohanizadeh & LeGeros 2007). Indirect evidence of the possibly good preservation of 500 Ma old brachiopod shell apatite is provided by XRD data (Fig. 7) that show a rather high variability of the lattice parameters of phase 2 (apatite phase from compact laminae) in comparison with phase 1 (from baculate laminae). Similar variability characterizes also the apatite unit cell dimensions in modern lingulids, where it can possibly be related to small specimen-specific variations in shell apatite chemistry (see section 2.1.1.). On the other hand, this variation could also be caused by the diagenetic changes affecting individual shells differently, as suggested for subfossil discinids

(Puura & Nemliher 2001). Possible recrystallization is also indicated by substitutions in cationic sites of the apatite crystal lattice, where Ca is partly substituted by Na and Mg, as in modern lingulids, which, however, contain more Mg than Na (Forchielli *et al.* 2014). Additionally, the EDS measurements suggest that the differences between Na and Mg in the apatite phases in compact and baculate laminae are only minor. Considering the previous discussion, it can be concluded that in addition to the preservation of apatite morphology in compact laminae, also the original apatite chemistry may in part be preserved, at least in shells of Furongian age.

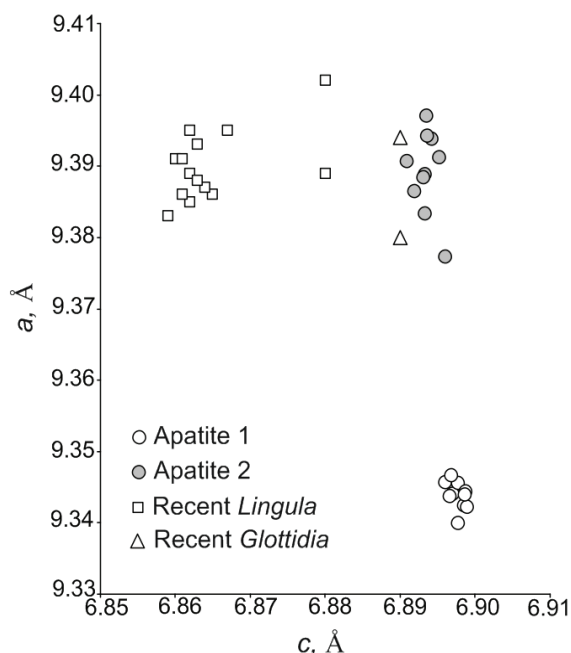


Figure 7. Variation in unit cell parameters a and c in Apatite phase 1 and Apatite phase 2 in *Ungula ingraca* (TUG 1323-5) and in modern *Lingula anatina* and *Glottidia pyramidata* (Watabe & Pan 1984; LeGeros *et al.* 1985; Iijima & Moriwaki 1990; Iijima *et al.* 1991; Zezina *et al.* 1993; Puura & Nemliher 2001). (Modified after Fig. 2 in Paper IV, values of *Glottidia pyramidata* added).

Apatite in baculate laminae, on the other hand, has a different chemico-structural composition than the apatite phase in compact laminae. Apatite in baculate laminae is morphologically represented by needle- or lath-shaped crystallites and is therefore interpreted as diagenetically recrystallized (e.g. Cusack & Williams 1996; Williams & Cusack 1997, 1999; Williams *et al.* 1998; Cusack *et al.* 1999). The results of ATR and EDS mapping presented in this thesis show that apatite in baculate laminae is rich in carbonate, calcium

and fluorine and has low (and fairly constant) XRD lattice parameter a values (Fig. 7) that may indicate the influence of the surrounding sedimentary environment (e.g. Stathopoulou *et al.* 2008). The apatite phase in baculate laminae is also characterized by a strong IR band at 864 cm^{-1} . The carbonate IR band at 864 cm^{-1} , instead of 872 cm^{-1} as in compact laminae, is probably linked to the high fluorine content and/or specific crystallo-chemical changes in this apatite phase (Fleet 2009; Yi *et al.* 2013). Whereas the IR band at 864 cm^{-1} is common in fossil skeletal apatites (e.g. Stathopoulou *et al.* 2008), it has been suggested that this band could be used as an indicator of diagenetic changes in bioapatites (Yi *et al.* 2013). The explicit origin of this phase, however, is not clear at this point. It could have been formed through the phosphatization of organics; secondary apatite could have been added through the bacterial degradation of shell organics or during some later phosphogenetic event. Furthermore, due to the porous nature of baculate laminae, the secondary apatite already formed as well as original shell apatite in baculate laminae could have been recrystallized at some point of the diagenetic history of these sediments. Moreover, it cannot be excluded that several of these processes may have played a role in the formation of the apatite phase in baculate laminae.

6.2. Nature and origin of nanofibrils (Papers I–III)

Narrow fibrils, so-called nanofibrils, are present in most of the studied brachiopod valves. Based on their characteristics (see section 5.1.2., Fig. 4) and assumed chemico-structural similarities with modern brachiopods, nanofibrils are interpreted here as a phosphatized fibrillar network, which may have been nonmineralized at the lifetime of the brachiopods (Papers II, III).

Mineralized rods, bacula, in modern lingulids have quite different diameters. For example, in *Glottidia palmeri* bacula are about 400 nm and in *Glottidia pyramidata* up to 750 nm in diameter (Cusack *et al.* 1999; Williams & Cusack 2007). These bacula, however, are aggregated around an axial biopolymer with the diameter of about 80–250 nm. For example, in modern *Glottidia pyramidata* and in Permian *Glottidia?* sp. its diameter is about 150 nm (Cusack *et al.* 1999 Pl. 4 fig. 4 and Pl. 8 fig. 5), in Silurian *Pseudolingula lewisii* about 250 nm (Cusack *et al.* 1999 Pl. 7 fig. 7) and in the oldest discinid *Schizotreta* (Williams *et al.* 1998) about 80 nm (Williams & Cusack 1999 Fig. 6h). Thus, from the size perspective, the nanofibrils with diameters of about 100–200 nm are rather comparable to the axial organic cores of bacula. The original organic composition of nanofibrils is further supported by their occasional curved shape (Fig. 4A, D), suggesting that the fibrils were flexible at the lifetime of the brachiopod. It is therefore possible that at least part of the nanofibrils represent the axial organic cores of bacula preserved through rapid phosphatization.

The phosphatization of organics has been documented in linguliform brachiopod valves also in previous works describing the preservation of membranous laminae (Williams & Cusack 1996; Cusack & Williams 1997;

Balthasar 2007) and possible preservation of collagen (Williams & Cusack 1996; Holmer & Bengtson 2009; Holmer & Nakrem 2012). Axial organic fibrils inside the bacula, however, are usually not preserved, instead an empty channel is observed inside the bacula of fossil shells (e.g. Cusack *et al.* 1999 Pl. 7 fig. 7; Cusack *et al.* 1999 Pl. 8 fig. 5; Williams & Cusack 1999 Fig. 6h). Degradation experiments with modern linguliforms have shown that the axial cores of bacula are probably proteinaceous (Williams & Cusack 2007) and are composed of amino acids such as glutamic acid, glycine, alanine, arginine and proline (Cusack *et al.* 1999). In order to be preserved in fossilized state, the proteins need to be rapidly phosphatized before they degrade (e.g. Allison 1988a,b; Butterfield 2003). This would be possible if the proteins had the composition that attracts the precipitating mineral ions (Butterfield 2003). The absence of a (strongly) mineralized cover in nanofibrils (Fig. 4) probably facilitates their phosphatization, while in mineralized bacula the organic core would be degraded as the mineral cover would not let the dissolved phosphate reach the axial fibril before it degrades (Fig. 8).

Bacula in the valves studied in this thesis are mostly recrystallized and their original size cannot probably be evaluated precisely. It is, however, evident (Figs 2, 3B), that the baculate laminae closer to shell exterior contain wider rod-like bacula, while towards the shell interior the bacula become (gradually) thinner and nanofibrils start to appear. The nanofibrils found in baculate laminae closer to shell interior are preserved either without a recrystallized cover or have only scarce needle/lath-like apatite crystallites sporadically attached to them, whereas the bacula in the external baculate laminae are often tightly covered by long prismatic apatitic needles (Figs 3, 4). It is therefore likely that at the lifetime of the studied linguliforms, the bacula (and inter-baculate spaces) closer to valve exterior were already more strongly mineralized. With the growing age of the brachiopod the younger baculate laminae became less mineralized and the areas where the bacula were non-mineralized became more frequent. This situation would not be much different from the valve mineralization in modern linguliforms. Non-mineralized fibrils (non-mineralized 'bacula') have also been documented in modern *Glottidia* (Iwata 1982 Fig. 1) where different baculate laminae are possibly also differently mineralized (Cusack *et al.* 1999 Text-fig. 5; Pl. 6 fig. 2).

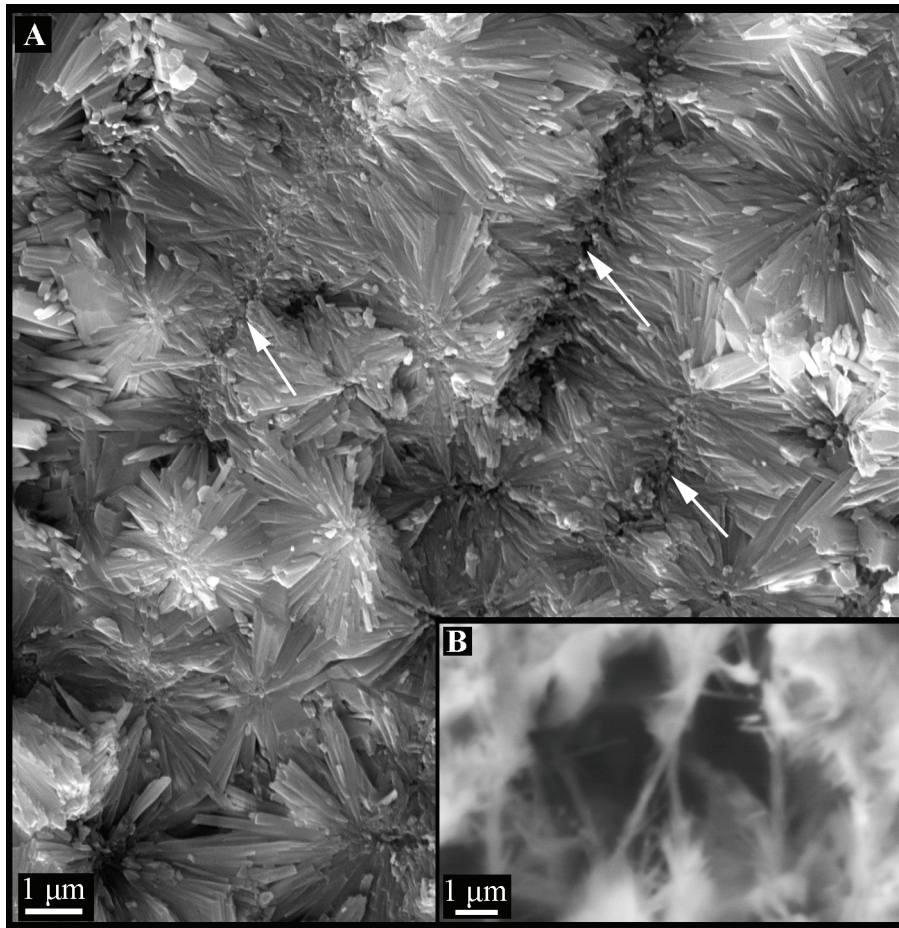


Figure 8. Strongly mineralized bacula (A; GIT 275-276 supplementary (unpublished) image) and phosphatized nanofibrils (B; TUG 1386-1 Paper II Fig. 3A) in baculate laminae of *Obolus ruchini*. The SEM-SE image of strongly mineralized bacula exposes their axial canals (arrows), which are about the same size as the diameter of phosphatized fibrils (SEM-BSE image, B).

Bacula becoming gradually thinner in younger baculate laminae can be observed also in Furongian *Obolus apollinis* (Cusack *et al.* 1999 Pl. 6 fig. 7; Nemliher *et al.* 2004 Fig. 5; Williams & Cusack 1999 Fig. 6a), in Silurian *Orbiculoidea forbesi* (Williams *et al.* 1998 Fig. 19b), in Cretaceous *Lingularia? notalis* (Holmer & Bengtson 2009 Fig. 4G), possibly also in Ordovician *Acrosaccus* sp. (Bassett *et al.* 1999 Figs 5–9). Possible explanation of such an effect can lie in the preferential mineralization of compact laminae, which are more frequent in the interior parts of the valve. Different proportions of mineralized and organic parts in certain sections of the shell may be relevant in the context of adaptive strategies, e.g. elasticity versus shell strength (Merkel *et al.* 2009).

Nanofibrils, thus, probably represent the early stages in the formation of bacula and in this way are relevant structural units in the hierarchical structure of Palaeozoic linguliform brachiopods. This also suggests that the development of bacula has not much changed during brachiopod evolution. Since at least Cambrian Epoch 3 (former ‘Middle Cambrian’) the bacula have formed through the aggregation of apatite on the axial fibrous organics. Larger bacula may additionally be formed from several fibrils bound together and covered with apatite as seen in the shells of *Obolus ruchini* (Paper II).

6.3. Variation in baculate shell structures (Papers I–III)

The shell structure of linguliform brachiopods is of phylogenetic significance (e.g. Cusack *et al.* 1999). The main shell structure types differentiated are baculate shell structure (characteristic of the order Lingulida), columnar shell structure (characteristic of and well studied in order Acrotretida; but also known from the order Paterinida and many brachiopod-like fossils) and virgose/botryoidal shell structure (characteristic of modern *Lingula*) (Williams & Cusack 1999). The columnar structure occurring in acrotretids (order Acrotretida) is well studied and according to present knowledge does not vary much within this order. The order Lingulida, on the other hand, is more varied with respect to shell structure: in addition to the prevailing baculate shell structure, also columnar and virgose structures have been found. Moreover, species of the genus *Eoobolus* may have different shell structures (Skovsted & Holmer 2005; Balthasar 2007, 2009; Streng *et al.* 2008; Ushatinskaya 2012; Ushatinskaya & Korovnikov 2014). In addition to that, baculate shell structure was recently divided into two sub-categories: the more prevailing inclined baculate structure and orthogonal baculate structure presently known in only five genera (Streng *et al.* 2008; Skovsted & Peel 2010). Baculate shell structures of fossil and modern linguliforms are also different, being baculate asymmetrical in modern lingulids but baculate symmetrical in most of fossil linguliforms (Williams & Cusack 1999). The discussion above shows that the shell structures in fossil lingulids have higher variability than previously acknowledged.

Shell structure studies presented in this thesis (Papers I–III) characterize the intergeneric variations in the genera *Obolus*, *Ungula* and *Bicarinatina*. Based on the classification by Popov *et al.* (1989) and the *Treatise on Invertebrate Paleontology*, the genus *Obolus* comprises three species: *O. apollinis*, *O. ruchini* and *O. transversus*. Three species are assigned also to the genus *Ungula*: *U. convexa*, *U. inornata* and *U. ingrlica*. The systematic revision of the genus *Bicarinatina* by the author of this thesis has revealed that this genus includes four species: *B. bicarinata*, *B. kongakutensis*, *B. wilsoni* and *B. indicis* (Paper I).

Cusack *et al.* (1999) have chosen *Obolus apollinis* (type species of the genus ***Obolus***) to typify the baculate symmetrical shell structure of fossil lingulids. In

O. apollinis (Cusack *et al.* 1999, Pl. 6, figs 3, 4, 6–8; Williams & Cusack 1999 Fig. 6; 2007, Figs 1592–1593) baculate laminae are formed of apatitic rods (bacula), which are about 500 nm in diameter, composed of prismatic apatite and arranged in a trellised way. Baculate laminae are subtended between two compact laminae, each about 2 μm thick. The maximum observable thickness of the outermost baculate lamina is 150 μm . Popov & Holmer (2003, Fig. 6E–F) illustrate fine criss-crossed bacula of *O. apollinis* that are about 400 nm thick. Nemliher *et al.* (2004, Fig. 5) show baculate laminae in a valve of *O. apollinis* treated with 5% H_2O_2 , which are 2–35 μm thick and contain bacula from about 500 nm to more than 1 μm in diameter. A close-up of baculate sets in *O. apollinis* published in Lang *et al.* (2011, Paper II Fig. 2A) reveals criss-crossed bacula about 1 μm in thickness and covered with spherulitic apatite aggregates. No published images of nanostructures of *O. apollinis* are available. Another representative of the genus *Obolus* studied in this thesis (Paper II), *O. ruchini*, reveals the presence of nanofibrils as well as bacula variously affected by diagenesis in the same shell and thus exposing bacula covered with prismatic apatite aggregates and measuring more than 1 μm in diameter (Fig. 3E, F). Criss-cross arrangement is not well developed in rod-like bacula that are rather vertical. No published images of the shell structural details are available for the third species assigned to the genus *Obolus* – *O. transversus*.

The type species of the genus *Ungula*, *U. convexa*, has coarse compactly placed bacula usually exceeding 1 μm in thickness (Popov & Holmer 2003 Fig. 6B, C), possibly due to the recrystallization of original shell apatite into spherulitic aggregates. Compact laminae in this species also are usually wider than in *Obolus* (Popov & Holmer 2003). The shell structure of *U. ingrlica* has been found to be rather homogeneous in early SEM studies, and different methods of etching have been used to reveal the shell structure. Holmer (1989 Fig. 14) illustrates fine bacula exposed on the etched surface of a valve of *U. ingrlica*. These bacula are about 350 nm wide, whereas their length can be more than 10 μm . The bacula have usually criss-crossed arrangement (Holmer 1989 Fig. 14), but may also be vertical, with a diameter more than 1 μm due to recrystallization (Fig. 3D). Compact laminae in this species have variable thicknesses and can be several tens of micrometres wide (Holmer 1989 Fig. 14B, D; Paper IV). Nanostructures have not been described from either *U. convexa* or *U. ingrlica*. The third species assigned to the genus *Ungula*, *U. inornata* studied in this thesis (Paper III), has up to 140 μm long and 3 μm thick bacula in the outermost baculate lamina, about 20 μm long and 1 μm thick bacula in the central baculate laminae and occasional nanofibrils less than 200 nm thick in the lower baculate laminae. The disposition of bacula is varying from inclined (criss-crossed) to vertical. A fragment of the baculate set of *U. inornata* is illustrated also in Cusack *et al.* (1999 Pl. 6, fig. 9) exposing coarse trellised more than 1 μm thick bacula.

The type species of the genus *Bicarinatina*, *B. bicarinata*, has baculate symmetrical shell structure with rod-like bacula 250–500 nm in diameter in outer baculate laminae of the valves and occasionally curved nanofibrils in the

inner baculate laminae (Papers I, II). Compact laminae of this species are 0.5–2.5 μm thick and better developed closer to the interior side of the valve (Paper I). Cusack *et al.* (1999 Text-fig. 3G) illustrate a fragment of a valve of Carboniferous *B. wilsoni* exposing baculate sets with criss-cross arrangement of bacula. They further describe that the bacula are composed of spherular apatite particles and are more than 1 μm in diameter. Information about the shell structure of the other two species included in the genus *Bicarinatina* is not available.

The characteristics that vary in baculate shell structure are the thickness (diameter) of bacula, orientation (inclination) of bacula, existence of axial threads (central channels) in bacula and relationship of bacula to compact laminae (e.g. Cusack *et al.* 1999). Because baculate laminae are more prone to post-mortem diagenetic changes, the original diameter of bacula may change substantially. In addition to that, the bacula likely have different lifetime diameters within the shell. The size of bacula in modern *Glottidia* and discinids remains below 1 μm , being larger in *Glottidia* and smaller in discinids. Diagenetically changed bacula are often more than 1 μm thick, however, also bacula thinner than 1 μm may be diagenetically strongly altered, so that their original diameter cannot be correctly identified. The diameter of bacula is changing also within a genus in modern lingulids (e.g. *Glottidia*).

The orientation (inclination) of bacula is highly variable in modern and fossil lingulids, occasionally varying from vertical to nearly horizontal even within the same valve (Williams & Cusack 1999). The variations in inclination seem to be partly due to changes in the speed of shell secretion, partly genetically controlled. Vertical and inclined, clearly criss-crossed bacula are believed to have been secreted differently (Williams & Cusack 2007). As vertical and inclined bacula may occur together in the same cross-section of the shell, this feature has obviously no strict genetic control. Some species, however, may secrete more regular baculate laminae, e.g. *O. apollinis* typically exposes inclined trellised bacula in the cross section of the shell. Secretion of such bacula may have been more strongly genetically controlled than the secretion of more vertical bacula. However, as the information about shell structure of half of the known lingulid genera is still lacking, we do not have a full picture of variations in baculate shell structures in lingulids.

The presence of the axial core is typical of bacula of modern lingulids and several works have revealed an axial channel also in bacula of fossil lingulids (e.g. Williams *et al.* 1998; Cusack *et al.* 1999; Williams & Cusack 1999; 2007). The core has a relatively constant size, being about 100–200 nm in diameter. In fossils it can be recognized as an empty channel inside the bacula or as phosphatized nanofibrils of the same size as the channels (Papers I–III; Fig. 8). The core, however, may be lacking in the orthogonal baculate shell structure type (Streng *et al.* 2008). The presence of a 100–200 nm thick axial core (channel, nanofibrils) is thus likely an important characteristic of the inclined baculate shell structure type.

The above discussion shows that (inclined) baculate shell structure is quite variable in modern and fossil lingulids, on the generic level as well as within a

single shell. The overall shell structure of the species belonging to the genera *Obolus*, *Ungula* and *Bicarinatina* is, however, rather similar. The most stable structural elements in (inclined) baculate shell structure seem to be the central channels (or nanofibrils) of bacula with the size of 100–200 nm. The mineralization of bacula varies throughout the laminae in the same shell and can be strongly modified by diagenesis. Early Palaeozoic lingulids probably had quite loose control on the secretion of bacula, with possible variations in the inclination of bacula. The same may be true for the mineralization of different parts of mineral and organic shell material in baculate laminae. This agrees well with the knowledge about modern linguliforms, where shell organics are suggested to have a rather directing, not strongly controlling role in shell mineralization (Neary *et al.* 2011). Rather weak biological control over shell apatite secretion is also suggested by the compositional variability of apatite within the same shell, between specimens of the same species and among different genera (see section 2.1.1.). Such flexibility in shell secretion may be one of the reasons why linguliforms with the baculate shell structure type have survived so well in geologic history.

6.4. Diagenesis (Papers I–IV)

When assessing diagenetic changes in brachiopod shell apatite, it is important to take into consideration that brachiopod shell apatite differs from vertebrate apatite. Original brachiopod shell apatite is carbonate-fluor apatite-like mineral (francolite), whereas vertebrate bioapatite represents a hydroxyapatite-like phase (Neary *et al.* 2011). In addition, unlike in bone, there is no strong physico-chemical interaction between mineral and organic matrix in the brachiopod shell, but the shell organics have a rather directing (Neary *et al.* 2011) and mineralizing (Lévêque *et al.* 2004) role in the secretion of shell apatite. Brachiopod shell apatite is thus crystalline and the crystals are relatively large (~50 nm, Schmahl *et al.* 2008). Taking the above into account and because the carbonate-fluor apatites are common and stable apatites in marine environments (Jahnke 1984; McClellan & van Kauwenbergh 1991; Knudsen & Gunter 2002), brachiopod shell apatite is apparently already a (more) stable mineral phase. This is also confirmed by shell minerals preserved in nanometric detail in Cretaceous *Lingula* (Cusack & Williams 1996).

On the other hand, brachiopod shell apatite seems not to be completely resistant to diagenetic change, as indicated by the presence of various prismatic apatite crystallites and aggregates (dumbbells, spherulites) in shell laminae (e.g. Cusack & Williams 1996; Papers I–IV). Since the prismatic crystallites and aggregates are found primarily in baculate laminae, they can complicate the interpretation of brachiopod shell structures by completely filling up the porous laminae as seen in *Ungula ingraca* used in this study (Paper IV) or in ‘Middle’ Cambrian *Lingulella* (Pettersson Stolk *et al.* 2010). Strong diagenetic alteration can also cause anomalous structures, e.g. in Lower Ordovician *Volborthia* (Holmer & Popov 1995), where

bacula are about 5 μm across. Furthermore, not everything that is mineralized in a fossil was mineralized at the brachiopod lifetime (Balthasar 2007). It is thus important to understand the diagenetic changes in shells, in order to correctly interpret the phylogenetically important shell structures as well as to assess the possible preservation of original valve chemistry.

The valves used in this study (Papers I–IV) show similar diagenetic status. Prismatic apatite crystallites and aggregates are common, but also apatite crystallites with the size and morphology similar to those of modern valves, and possible phosphatization of originally organic components are present. The diagenesis of linguliforms is therefore a complex process that possibly has several stages. Based on the data obtained for this thesis, a general description of the successive diagenetic stages that may affect linguliform shells can be compiled (Fig. 9).

1. Phosphatization (Fig. 9-1). Labile shell organics are the first that start to degrade during early post-mortem processes, releasing the elements needed for rapid phosphatization of nanofibrils (Papers I–III). With progressing organic decay various diagenetic environments are formed in the shell (Papers II, III; Balthasar 2007).

2. Stabilization of original bioapatite (Fig. 9-2). If the organics around bioapatite are degraded, the original biological environment in which the crystallites were stable, changes. This increases the thermodynamic disequilibrium between bioapatite and the new geochemical environment, which necessitates stabilization of the original bioapatite to the new environment. In case of brachiopod apatite, the stabilization leads to either the preservation of spherical apatite particles morphologically and partly also chemically, similar to the apatite in modern linguliform shells (Paper IV), or to the formation of prismatic apatite crystallites and aggregates found primarily in baculate laminae (Papers II–IV). It is not clear how the stabilization processes proceed. Unstable phases may recrystallize, dissolve and/or new authigenic phases may grow (e.g. Trueman 2013). In case of bone apatite, for example, it is suggested that the stabilization during diagenesis may result from coupled dissolution–reprecipitation processes (Pasteris & Ding 2009), which may also preserve the original crystal size and orientation (Putnis 2009; see also Herwartz *et al.* 2013 annex 1 for a review about fossilization of biogenic apatite). The stabilization phase is likely related to the amount of organics and the compactness in the arrangement of apatite crystals. There is a clear difference in both crystal morphology and chemistry in originally organic-rich baculate laminae and in compact laminae that contain originally less organics and where apatite crystals are more compactly arranged (Paper IV). A similar dependence of the amount of organics and crystal arrangements has been noted also for vertebrate and conodont apatites (e.g. Kohn & Cerling 2002; Trotter & Eggins 2006). Compact laminae of linguliforms may thus preserve some of their original composition, at least in their central parts that are not directly connected to organic-rich baculate laminae (Paper IV).

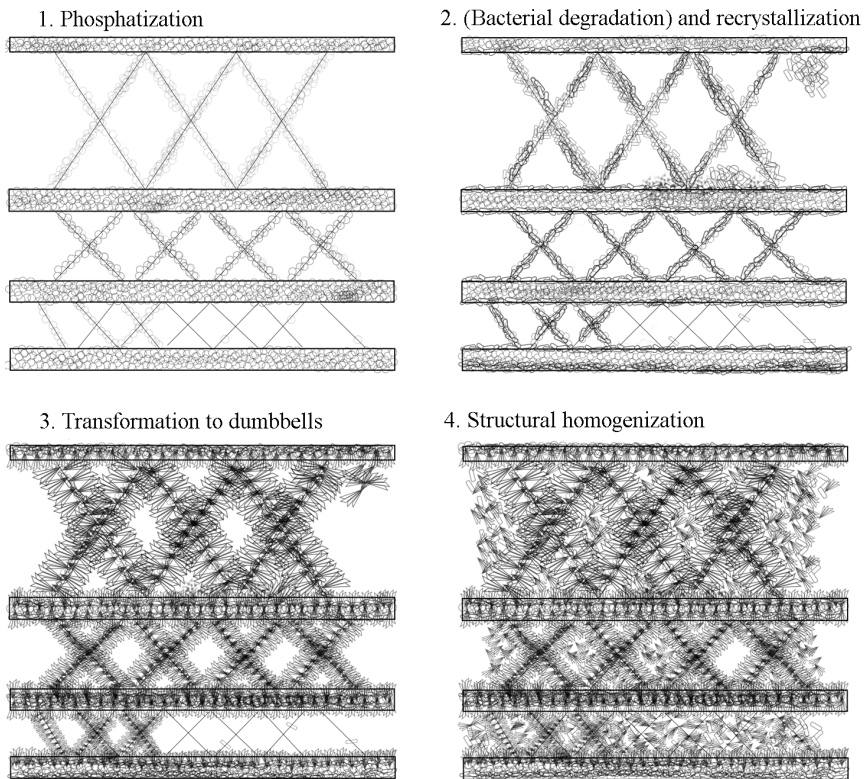


Figure 9. Scenario of diagenetic processes in linguliform shells. The original shell is composed of aggregates of spherical apatite particles (mostly ellipsoids) enmeshed in organic matrix. 1) Phosphatization – selective phosphatization of some fibrillar organics of the shell (and/or other types of shell organics); 2) stabilization – the spherical apatite particles and their aggregates initially turn into prismatic crystals; in case of bacterial degradation of organics also some authigenic pyrite and/or apatite could be precipitated in free pore space; 3) apatite transformations – the prisms turn into dumbbells (or fascicles if the growth is inhibited at one side of the crystal; fascicles may also form in the interbaculate space when dumbbells break into two halves) and further to spherulitic aggregates; 4) structural homogenization through the growth of prismatic apatite crystals originating from the recrystallization of original shell apatite and/or addition of authigenic apatite.

3. Apatite transformations (Figs 9-3; 10). During stabilization processes in more organic-rich areas in the shell (baculate laminae) greater diagenetic changes occur both in mineral morphology (Papers II–IV) and chemical composition (Paper IV). Changes in mineral morphology are associated with the pseudomorphic recrystallization of original apatite particles (Cusack & Williams 1996; Williams *et al.* 1998; Williams & Cusack 1999). Needle-like prisms are most common and

may have been formed through the recrystallization of originally linearly aligned spherical apatite particles (Cusack & Williams 1996). Apatite *in vitro* crystallization tests show that apatitic dumbbells form from prismatic seeds under specific conditions of pH (~5–7) and supersaturation (Peters & Epple 2001; Prymak *et al.* 2006), whereas their formation may be connected with the presence of organics. Dumbbells may further develop into spherulitic crystal aggregates (e.g. Prymak *et al.* 2006). Similar apatite transformations may have occurred also in linguliform brachiopod shells. During early diagenetic degradation of organics the pH of pore fluids would be lowered to about 5–7 and the shell apatite recrystallized into prismatic crystallites would further develop into dumbbells and spherulites (Papers II–III). Such development involves substantial change in the morphology and size of original shell apatite in a relatively short period of time (Bush *et al.* 1999), possibly due to authigenic apatite originating from organic decay. As such dumbbells or spherulitic aggregates are often grown on bacula, the original size of bacula may be largely changed.

4. Structural homogenization (Fig. 9–4). If the diagenetic apatite aggregates grow large enough or if (locally) the supersaturation gets high enough to phosphatize large amounts of organics, the shell structures may be homogenized. This process finally leads to loss of the original shell structure (e.g. the areas closer to the valve exterior in *Obolus ruchini* in Paper II and *U. ingraca* in Paper IV).

Because of the variation in the thickness and organic content of baculate laminae in the valve cross section, the specific diagenetic conditions may change between different laminae and also within a single lamina (e.g. mid-parts of the laminae and valve margins, Balthasar 2007), causing microscale variation in supersaturation and pH. Several diagenetic stages may therefore be exposed in the same shell (e.g. *O. ruchini*, Paper II). Furthermore, diagenetic pyrite was often detected in the laminar structure of the brachiopod shells studied in this thesis. This suggests that some of the apatite in the baculate laminae could have been precipitated through bacterially mediated processes driven by sulphate-reducing bacteria degrading the organic tissues of the linguliforms under suboxic to anoxic conditions (Lécuyer *et al.* 1998). Bacterially mediated (enzymatic) hydrolysis of organic matter may substantially lower the oxygen isotope values in the incipient apatite crystals (e.g. Goldhammer *et al.* 2011), which in turn might suggest that the apatite in baculate laminae is unsuitable for palaeoenvironmental analyses. Interference of bacterially influenced apatite could also explain the typically low (about 15–16‰) phosphate $\delta^{18}\text{O}_{\text{PO}_4}$ values in fossil obolids (Lécuyer *et al.* 1998). This problem, however, needs further research.

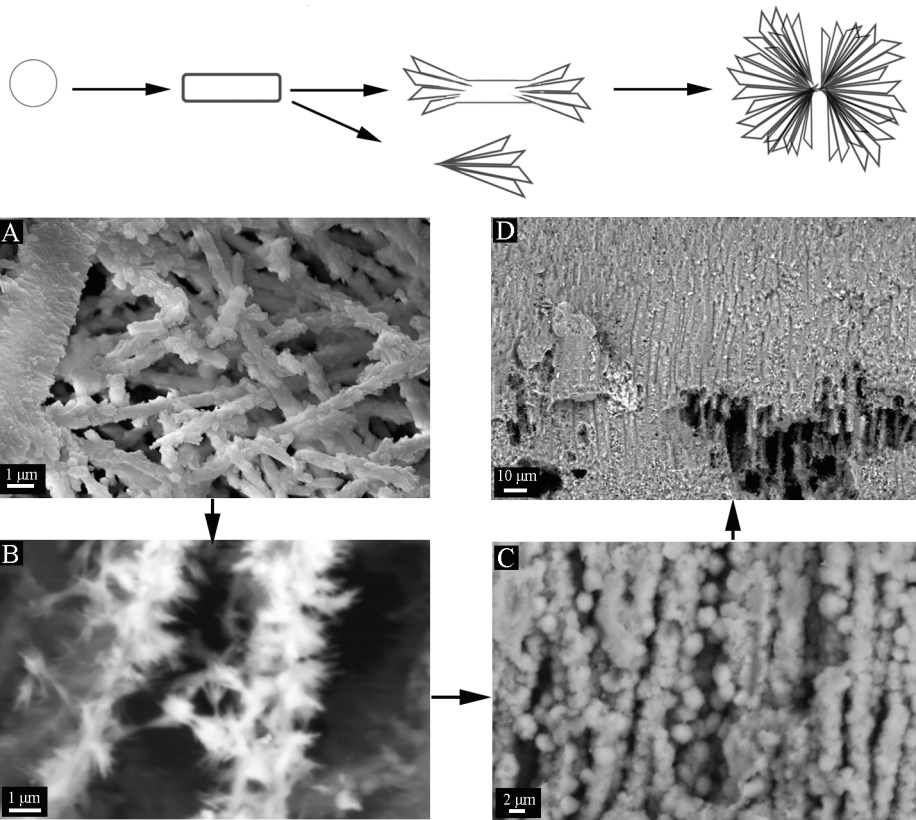


Figure 10. Transformation of shell apatite from spherical apatite particles to prisms, to dumbbells/fascicles, to spherulitic aggregates and structural homogenization. SEM images from the upper left image in the order shown by arrows: A) SEM-BSE image showing apatite starting to branch to dumbbells in the baculate lamina in a shell of *Obolus apollinis* (TUG 1323-10, additional unpublished image); the compact lamina near the left edge of this image is also covered with prismatic apatite crystallites, however, the central part of the lamina appears to be composed of spherical crystallites. B) Dumbbells in the shell of *Obolus ruchini* (TUG 1386-1, supplementary (unpublished) image related to Paper II). C) Spherulitic aggregates covering bacula in *Ungula inornata* (TUG 1323-4, Paper III Fig. 3G). D) Structural homogenization due to addition and/or growth of prismatic crystallites and aggregates on bacula in *Obolus ruchini* (TUG 1386-1, supplementary (unpublished) image related to Paper II).

7. CONCLUSIONS

In order to use linguliform brachiopod shells in phylogenetic and palaeo-environmental studies, the range of diagenetic changes in fossil shells should be considered. The diagenesis of linguliforms is a complex multistage process that is heterogeneous on a microscale. The following conclusions can be drawn from this study:

- The size and appearance of baculate laminae and bacula vary substantially throughout the studied fossil linguliform shells due to the variations in the degree of the *in vivo* mineralization of bacula. At later stages of shell secretion baculate laminae became thinner and less mineralized, which affected also the size of bacula.
- Younger baculate laminae often contain nanofibrils with a diameter of 100–200 nm. Nanofibrils were likely originally non-mineralized (organic) and were preserved by instant early post-mortem phosphatization. Nanofibrils represent the early stages in the formation of bacula. Similar morphologies of the nanostructures shaping the baculate structure in modern linguliforms suggest that the development of bacula has not changed much since at least Cambrian Epoch 3.
- Different diagenetic conditions may develop in different parts of the valve due to variations in the thickness and degree of the mineralization and organic content of separate shell laminae. Due to this heterogeneity, various diagenetic features may be exposed in the same fossil valve. The succeeding diagenetic stages are: phosphatization of organics, stabilization of original bioapatite, apatite transformations and structural homogenization.
- Prismatic apatite crystallites reflect the diagenetic change in fossil linguliforms. These crystallites may have further developed into dumbbells or spherulitic aggregates formed only under specific diagenetic conditions. These changes seem to be accompanied by authigenesis that substantially changes the shape/size of original bioapatite aggregates and may further complicate the interpretation of phylogenetically important structural elements.
- Even though shell apatite may be secreted as a relatively stable apatite phase, the results of chemical analyses show that the apatite composition of fossil shells is varying. Furthermore, chemical variations in fossil shell apatite of *Ungula ingraca* can be associated with compact and baculate laminae. Apatite in baculate laminae is rich in carbonate, fluoride and calcium, but has relatively less Na and Mg. Apatite in compact laminae has relatively less carbonate and fluoride anions and calcium is partly replaced by other cations (such as Na and Mg).
- The data obtained from ATR and EDS mapping allow us to locate the shell apatite phases previously known from powder XRD analyses. The apatite phase with higher XRD lattice parameter *a* values is located in compact

- laminae, while the apatite phase with lower a values occurs in baculate laminae.
- According to ATR-FTIR, SEM-EDS and XRD analyses, the apatite in compact laminae of *Ungula ingraca* shows both morphological and chemical similarities with shell apatite of modern linguliforms. The contents of CO_3^{2-} and F, XRD lattice parameter values and their variations, and the appearance of the carbonate IR band at 872 cm^{-1} are comparable with respective parameters in modern linguliform apatite. Slight recrystallization is indicated by variations in cation sites. This suggests that some of the biological or palaeoenvironmental information may have been preserved within the compact laminae of linguliforms of Furongian age.
 - Diagenetic changes in linguliform shell apatite lead to an increase in the carbonate and fluorine content, the appearance of the carbonate IR band at 864 cm^{-1} , low (and fairly constant) XRD lattice parameter a values and development of needle- or lath-like apatite crystallites. Such changes affect more strongly organic-rich baculate laminae and are associated with the (bacterial) degradation of shell organics. Altered shell apatite has only a limited potential for palaeoenvironmental analysis.

ACKNOWLEDGEMENTS

I wish to express my gratitude to my supervisors Prof. Tõnu Meidla and the late Dr. Ivar Puura for their guidance and support throughout my studies. My co-authors Prof. Kalle Kirsimäe, Signe Vahur (Institute of Chemistry, University of Tartu) and Ethel Uibopuu (now Tamm) are warmly thanked for inspiring discussions and helpful suggestions during various phases of my research. I am thankful to Prof. Aivo Lepland (Norwegian Geological Survey), Jaan Aruväli and Lauri Joosu for technical support, and Ursula Toom (Institute of Geology, Tallinn University of Technology) and Ivars Zupins (Latvian Museum of Natural History) for the help with museum materials needed for this study. Anne Noor is acknowledged for language correction.

This research was funded by the Estonian Science Foundation (grants 6460 and 8049) and Estonian Research Council (grants SF0180051s08 and IUT20-34). Additional financial support for early SEM analyses and attending the conferences was provided by Doctoral School of Ecology and Earth Sciences, the Archimedes Foundation (Kristjan Jaak mobility programme) and Sir Alwyn Williams Foundation.

Finally, I appreciate the support of my colleagues at the Department of Geology at the University of Tartu, especially ‘palaeo-colleagues’ Karin Truuver and Oive Tinn. I am deeply grateful for the support of my family and friends.

REFERENCES

- Allison, P. A. 1988(a): The role of anoxia in the decay and mineralization of proteinaceous macro-fossils. *Paleobiology* 14, 139–154.
- Allison, P. A. 1988(b): Konservat-lagerstätten: cause and classification. *Paleobiology* 14, 331–344.
- Antonakos, A., Liarokapis, E. & Leventouri, T. 2007: Micro-Raman and FTIR studies of synthetic and natural apatites. *Biomaterials* 28, 3043–3054.
- Aoba, T., Shimazu, Y., Taya, Y., Soeno, Y., Sato, K. & Miake, Y. 2003: Fluoride and apatite formation *in vivo* and *in vitro*. *Journal of Electron Microscopy* 52, 615–625.
- Balthasar, U. 2007: An Early Cambrian organophosphatic brachiopod with calcitic granules. *Palaeontology* 50, 1319–1325.
- Balthasar, U. 2009: The brachiopod *Eoobolus* from the Early Cambrian Mural Formation (Canadian Rocky Mountains). *Paläontologische Zeitschrift* 83, 407–418.
- Balthasar, U. & Butterfield, N. J. 2008: Early Cambrian “soft-shelled” brachiopods as possible stem-group phoronids. *Acta Palaeontologica Polonica* 54, 307–314.
- Balthasar, U., Skovsted, C. B., Holmer, L. E. & Brock, G. A. 2009: Homologous skeletal secretion in tomotiids and brachiopods. *Geology* 37, 1143–1146.
- Bassett, M. G., Popov, L. E. & Holmer, L. E. 1999: Organophosphatic brachiopods: patterns of biodiversification and extinction in the Early Palaeozoic. *Geobios* 32, 145–163.
- Bassett, D., Macleod, K. G., Miller, J-F. & Ethington, R. L. 2007: Oxygen isotopic composition of biogenic phosphate and the temperature of Early Ordovician seawater. *PALAIOS* 22, 98–103.
- Bush, S., Dolhaine, H., DuChesne, A., Heinz, S., Hochrein, O., Laeri, F., Podebrad, O., Vietze, U., Weiland, T. & Kniep, R. 1999: Biomimetic morphogenesis of fluorapatite-gelatin composites: fractal growth, the question of intrinsic electric fields, core/shell assemblies, hollow spheres and reorganization of denatured collagen. *European Journal of Inorganic Chemistry*, 1643–1653.
- Butterfield, N. J. 2003: Exceptional fossil preservation and the Cambrian Explosion. *Integrative and Comparative Biology*. 43, 166–177.
- Cusack, M. & Williams, A. 1996: Chemico-structural degradation of Carboniferous lingulid shells. *Philosophical Transactions of The Royal Society B: Biological Sciences* 351, 33–49.
- Cusack, M. & Williams, A. 2007: Biochemistry and diversity of brachiopod shells. In Selden, P. A. (ed.): *Treatise on Invertebrate Paleontology. Part H, Brachiopoda, Revised 6*. Geological Society of America & Paleontological Institute, pp. 2373–2395. Boulder, Colorado, & Lawrence, Kansas.
- Cusack, M., Williams, A. & Buckman, J. O. 1999: Chemico-structural evolution of linguloid brachiopod shells. *Palaeontology* 42, 799–840.
- Dahm, S. & Risnes, S. 1999: A comparative infrared spectroscopic study of hydroxide and carbonate absorption bands in spectra of shark enameloid, shark dentin, and a geological apatite. *Calcified Tissue International* 65, 459–465.
- Eichwald, E. 1829: *Zoologia specialis, quam expositis animalibus tum vivis, tum fossilibus potissimum Rossiae in universum et Poloniae in specie*, in usum lectionum publicarum Universitate Caesarea Vilnesi 1, 314 pp. Josephi Zawadski, Vilnae.
- Elliott, J. C. 2002: Calcium phosphate biominerals. In Kohn, M. J., Rakovan, J. & Hughes, J. M. (eds): *Phosphates: geochemical, geobiological, and materials importance. Reviews in Mineralogy and Geochemistry* 48, 427–453.

- Emig, C. C., Bitner, M. A. & Álvarez, F. 2013: Phylum Brachiopoda. In Zhang, Z.-Q. (ed.) Animal biodiversity: an outline of higher-level classification and survey of taxonomic richness (Addenda 2013) *Zootaxa* 3703, 075–078.
- Emig, C. C., Álvarez, F., Bitner, M. A. 2015: *World Brachiopoda database*. Accessed at <http://www.marinespecies.org/brachiopoda> on 2015-04-25.
- Fleet, M. E. 2009: Infrared spectra of carbonate apatites: ν_2 -Region bands. *Biomaterials* 30, 1473–1481.
- Fleet, M. E. & Liu, X. 2008: Accommodation of the carbonate ion in fluorapatite synthesized at high pressure. *American Mineralogist* 93, 1460–1469.
- Forchielli, A., Steiner, M., Hu, S., Lüter, C. & Keupp, H. 2014: Taphonomy of the earliest Cambrian linguliform brachiopods. *Acta Palaeontologica Polonica* 59, 185–207.
- Goldhammer, T., Brunner, B., Bernasconi, S. M., Ferdelman, T. G. & Zabel, M. 2011: Phosphate oxygen isotopes: insights into sedimentary phosphorous cycling from the Benguela upwelling system. *Geochimica et Cosmochimica Acta* 75, 3741–3756.
- Herwartz, D., Tütken, T., Johum, K. P. & Sander, P. M. 2013: Rare earth element systematics of fossil bone revealed by LA-ICPMS analysis. *Geochimica et Cosmochimica Acta* 103, 161–183.
- Holmer, L. 1989: Middle Ordovician phosphatic inarticulate brachiopods from Västergötland and Dalarna, Sweden. *Fossils and Strata* 26, 1–172.
- Holmer, L. E. & Bengtson, P. 2009: The first occurrence of a lingulid brachiopod from the Cretaceous of Sergipe, Brazil, with a restudy of “*Lingula*” *bagualensis* Wilckens, 1905 from southern Patagonia. *Paläontologische Zeitschrift* 83, 255–266.
- Holmer, L. E. & Nakrem, H. A. 2012: The lingulid brachiopod *Lingularia* from lowermost Cretaceous hydrocarbon seep bodies, Sassenfjorden area, central Spitsbergen, Svalbard. *Norwegian Journal of Geology* 92, 167–174.
- Holmer, L. E. & Popov, L. E. 1995: The elkaniide brachiopod *Volborthia* from the Lower Ordovician of Baltoscandia. *Paläontologische Zeitschrift* 69, 213–221.
- Holmer, L. E. & Popov, L. E. 2007: Linguliformea. In Selden, P.A. (ed.) Treatise on invertebrate paleontology Part H Brachiopoda Revised. Vol. 6, 2355–2590. The Geological Society of America, Inc. and The University of Kansas. Boulder, Colorado and Lawrence, Kansas.
- Holmer, L. E., Popov, L. & Streng, M. 2008: Organophosphatic stem group brachiopods: implications for the phylogeny of the subphylum Linguliformea. *Fossils and Strata* 54, 3–11.
- Hughes, J. M. & Rakovan, J. 2002: The crystal structure of apatite, $\text{Ca}_5(\text{PO}_4)_3(\text{F},\text{OH},\text{Cl})$. In Kohn, M. J., Rakovan, J. & Hughes, J. M. (eds): *Phosphates: geochemical, geobiological, and materials importance*. *Reviews in Mineralogy and Geochemistry* 48, 1–12.
- Igisu, M., Komiya, T., Kawashima, M., Nakashima, S., Ueno, Y., Han, J., Shu, D., Li, Y., Guo, J., Maruyama, S. & Takai, K. 2014: FTIR microspectroscopy of Ediacaran phosphatized microfossils from the Doushantou Formation, Weng’an, South China. *Gondwana Research* 25, 1120–1138.
- Iijima, M. & Moriwaki, Y. 1990: Orientation of apatite and organic matrix in *Lingula unguis* shell. *Calcified Tissue International* 47, 237–242
- Iijima, M., Kamemizu, H., Wakamatsu, N., Goto, T. & Moriwaki, Y. 1991: Thermal decomposition of *Lingula* shell apatite. *Calcified Tissue International* 49, 128–133.

- Iwata, K. 1982: Ultrastructure and calcification of the shells in inarticulate brachiopods Part 2. Ultrastructure of the shells of *Glottidia* and *Discinisca*. *Journal of the Geological Society of Japan* 88, 957–966 (in Japanese with English abstract).
- Jahnke, R. A. 1984: The synthesis and solubility of carbonate fluorapatite. *American Journal of Science* 284, 58–78.
- Khazanovitch, K. K., Popov, L. E. & Melnikova, L. M. (eds). 1984: Bezzamkovye brachiopody, ostrakody (bradoriidy) i khiolitel'minty iz sablinskoj svity Leningradskoj oblasti [Inarticulate brachiopods, ostracodes (bradoriids) and hyolithelminths from the Sablinka Formation of the Leningrad District]. *Paleontologicheskij Zhurnal* 1984, 33–47 (in Russian).
- Knoll, A. H. 2003: Biomineralization and evolutionary history. In Dove, P., De Yoreo, J. & Weiner, S. (eds): *Biomineralization. Reviews in Mineralogy and Geochemistry* 54, 329–356.
- Knudsen, A. C. & Gunter, M. E. 2002: Sedimentary phosphorites – An example: Phosphoria Formation, Southeastern Idaho, U.S.A. In Kohn, M. J., Rakovan, J. & Hughes, J. M. (eds): *Phosphates: geochemical, geobiological, and materials importance. Reviews in Mineralogy and Geochemistry* 48, 363–389
- Kohn, M. J. & Cerling, T. E. 2002: Stable isotope composition of biological apatites. In Kohn, M. J., Rakovan, J. & Hughes, J. M. (eds): *Phosphates: geochemical, geobiological, and materials importance. Reviews in Mineralogy and Geochemistry* 48, 455–488.
- Kouchinsky, A., Bengtson, S., Runnegar, B., Skovsted, C., Steiner, M. & Vendrasco, M. 2012: Chronology of early Cambrian biomineralization. *Geological Magazine* 149, 221–251.
- Kutorga, S. 1837: *Zweiter Beitrag zur Geognosie und Paläontologie Dorpats und seiner nächsten Umgebungen*. St.-Petersbourg, 51 pp.
- Larsson, C. M., Skovsted, C. B., Brock, G. A., Balthasar, U., Topper, T. P. & Holmer, L. E. 2014: *Paterimitra pyramidalis* from South Australia: scleritome, shell structure and evolution of a lower Cambrian stem group brachiopod. *Palaeontology* 57, 417–446.
- Lebon, M., Müller, K., Bahain, J.-J., Fröhlich, F., Falguères, C., Bertrand, L., Sandt, C. & Reiche, I. 2011: Imaging fossil bone alterations at the microscale by SR-FTIR microspectroscopy. *Journal of Analytical Atomic Spectrometry* 26, 922–929.
- Lécuyer, C., Grandjean, P., Barrat, J.-A., Nolvak, J., Emig, C., Paris, F. & Robardet, M. 1998: $\delta^{18}\text{O}$ and REE contents of phosphatic brachiopods: a comparison between modern and lower Paleozoic populations. *Geochimica et Cosmochimica Acta* 62, 2429–2436.
- Lécuyer, C., Grandjean, P. & Emig, C. C. 1996: Determination of oxygen isotope fractionation between water and phosphate from living lingulids: potential application to paleoenvironmental studies. *Palaeogeography, Palaeoclimatology, Palaeoecology* 126, 101–108.
- LeGeros, R. Z., Pan, C.-M., Suga, S. & Watabe, N. 1985: Crystallo-chemical properties of apatite in atremate brachiopod shells. *Calcified Tissue International* 37, 98–100.
- Lévêque, I., Cusack, M., Davis, S. A. & Mann, S. 2004: Promotion of fluorapatite crystallization by soluble-matrix proteins from *Lingula anatina* shells. *Angewandte Chemie International Edition* 43, 885–888.
- McClellan, G. H. & van Kauwenbergh, S. J. 1991: Mineralogical and chemical variation of francolites with geological time. *Journal of the Geological Society, London* 148, 809–812.

- Merkel, C., Deuschle, J., Griesshaber, E., Enders, S., Steinhauser, E., Hochleitner, R., Brand, U. & Schmahl, W. W. 2009: Mechanical properties of modern calcite- (*Mergerlia truncata*) and phosphate-shelled brachiopods (*Discradisca stella* and *Lingula anatina*) determined by nanoindentation. *Journal of Structural Biology* 168, 396–408.
- Merkel, C., Griesshaber, E., Kelm, K., Neuser, R., Jordan, G., Logan, A., Mader, W. & Schmahl, W. W. 2007: Micromechanical properties and structural characterization of modern inarticulated brachiopod shells. *Journal of Geophysical Research* 112, G02008.
- Mickwitz, A. 1896: Über die Brachiopodengettung *Obolus* Eichwald. *Memoires de l'Académie Impériale des Sciences de St. Pétersbourg* 4, 1–215.
- Neary, M. T., Reid, D. G., Mason, M. J., Frišćić, T., Duer, M. J. & Cusack, M. 2011: Contrasts between organic participation in apatite biomineralization in brachiopod shell and vertebrate bone identified by nuclear magnetic resonance spectroscopy. *Journal of the Royal Society Interface* 8, 282–288.
- Nemliher, J. 1999: Mineralogy of Phanerozoic skeletal and sedimentary apatites: an XRD study. *Dissertationes Geologicae Universitatis Tartuensis*. Tartu University Press. 135 pp.
- Nemliher, J., Kurvits, T., Kallaste, T. & Puura, I. 2004: Apatite varieties in the shell of the Cambrian lingulate brachiopod *Obolus apollinis* Eichwald. *Proceedings of the Estonian Academy of Sciences: Geology* 53, 246–256.
- Pan, Y. & Fleet, M. E. 2002: Composition of the apatite-group minerals: substitution mechanisms and controlling factors. In Kohn, M. J., Rakovan, J. & Hughes, J. M. (eds): *Phosphates: geochemical, geobiological, and materials importance. Reviews in Mineralogy and Geochemistry* 48, 13–49.
- Pasteris, J. D. & Ding, D. Y. 2009: Experimental fluoridation of nanocrystalline apatite. *American Mineralogist* 94, 53–63.
- Peters, F. & Epple, M. 2001: Crystallisation of calcium phosphates under constant conditions with a double diffusion set-up. *Journal of the Chemical Society, Dalton Transactions*, 3585–3592.
- Pettersson Stolk, S., Holmer, L. E. & Caron, J.-B. 2010: First record of the brachiopod *Lingulella waptaensis* with pedicle from the Middle Cambrian Burgess Shale. *Acta Zoologica (Stockholm)* 91, 150–162.
- Popov, L. E. & Holmer, L. E. 2003: Understanding linguloid brachiopods: *Obolus* and *Ungula* as examples. *Garnets de Géologie/Notebooks on Geology*, Maintenon, Article 2003/06 (CG2003_A06_LEP-LEH)
- Popov, L. E., Khazanovitch, K. K., Borovko, N. G., Sergeeva, S. P. & Sobolevskaya, P. F. 1989: Opornye razrezy i stratigrafiya kembro-ordovikskoj fosforitonoj obo- lovoj tolshchi na severo-zapade Russkoj platformy [The key sections and stratigraphy of the phosphate-bearing *Obolus* beds in the north-east of the Russian Platform]. *AN SSSR, Ministerstvo Geologii SSSR, Mezhdovedstvennyi Stratigraficheskij Komitet SSSR, Trudy* 18, 1–222 (in Russian).
- Prymak, O., Sokolova, V., Peitsch, T. & Epple, M. 2006: The crystallization of fluora- patite dumbbells from supersaturated aqueous solution. *Crystal Growth & Design* 6, 498–506.
- Putnis, A. 2009: Mineral replacement reactions. *Reviews in Mineralogy and Geochemistry* 70, 87–124.
- Puura, I. & Nemliher, J. 2001: Apatite varieties in Recent and fossil linguloid brachiopod shells. In Brunton, C. H., Cocks, L. R. M. & Long, S. L. (eds):

- Brachiopods past and present. The Systematics Association Special Volume Series 63*, 6–16.
- Reiche, I., Lebon, M., Chadeaux, C., Müller, K., Le Hô, A.-S., Gensch, M. & Schade, U. 2010: Microscale imaging of the preservation state of 5,000-year-old archaeological bones by synchrotron infrared microscopy. *Analytical & Bioanalytical Chemistry* 397, 2491–2499.
- Rintoul, L., Wentrup-Byrne, W., Suzuki, S. & Grøndahl, L. 2007: Ft-IR spectroscopy of fluoro-substituted hydroxyapatite: strengths and limitations. *Journal of Materials Science: Materials in Medicine* 18, 1701–1709.
- Rodland, D. L., Kowalewski, M., Dettman, D. L., Flessa, K. W., Atudorei, V. & Sharp, Z. D. 2003: High resolution analysis of $\delta^{18}\text{O}$ in modern and fossil lingulid brachiopods. *Journal of Geology* 111, 441–453.
- Rodríguez-Lorenzo, L. M., Hart, J. N. & Gross, K. A. 2003: Influence of fluorine in the synthesis of apatites. Synthesis of solid solutions of hydroxyl-fluorapatite. *Biomaterials* 24, 3777–3785.
- Rohanizadeh, R. & LeGeros, R. Z. 2007: Mineral phase in linguloid brachiopod shell: *Lingula adamsi*. *Lethaia* 40, 61–68.
- Schmahl, W. W., Griesshaber, E., Merkel, C., Kelm, K., Deuschle, J., Neuser, R. D., Göetz, A. J., Sehrbrock, A. & Mader, M. 2008: Hierarchical fibre composite structure and micromechanical properties of phosphatic and calcitic brachiopod shell biomaterials – an overview. *Mineralogical Magazine* 72, 541–562.
- Skovsted, C. B. & Holmer, L. E. 2005: Early Cambrian brachiopods from north-east Greenland. *Palaeontology* 48, 325–345.
- Skovsted, C. B. & Holmer, L. E. 2006: The Lower Cambrian brachiopod *Kyrshabaktella* and associated shelly fossils from the Harkless Formation, southern Nevada. *GFF* 128, 327–337.
- Skovsted, C. B. & Peel, J. S. 2010: Early Cambrian brachiopods and other shelly fossils from the basal Kinzers Formation of Pennsylvania. *Journal of Paleontology* 84, 754–762.
- Stathopoulou, S. T., Psycharis, V., Chryssikos, G. D., Gionis, V. & Theodorou, G. 2008: Bone diagenesis: new data from infrared spectroscopy and X-ray diffraction. *Palaeogeography, Palaeoclimatology, Palaeoecology* 266, 168–174.
- Streng, M. & Holmer, L. E. 2005: Discovery of a new shell structure within the organophosphatic brachiopods and the status of the family Curticiidae. *GFF* 127, 7–16.
- Streng, M., Holmer, L. E., Popov, L. E. & Budd, G. E. 2008: Columnar shell structures in early linguloid brachiopods – new data from the Middle Cambrian of Sweden. *Earth and Environmental Science Transactions of the Royal Society of Edinburgh* 98, 221–232.
- Zabini, C., Schiffbauer, J. D., Xiao, S. & Kowalewski, M. 2012: Biomineralization, taphonomy, and diagenesis of Paleozoic lingulid brachiopod shells preserved in silicified mudstone concretions. *Palaeogeography, Palaeoclimatology, Palaeoecology* 326–328, 118–127.
- Zeina, O. N., Nemliher, J. G., Rummi, P. & Ushatinskaya, G. T. 1993: Studies of the mineral component of the chitin-phosphate shells of Recent Brachiopods in connection with the specifics of deep-sea forms. *Okeanologiya* 33, 248–252 (in Russian), 212–216 (in English).
- Trotter, J. A. & Eggins, S. M. 2006: Chemical systematics of conodont apatite determined by laser ablation ICPMS. *Chemical Geology* 233, 196–216.

- Trueman, C. N. 2013: Chemical taphonomy of biomineralized tissues. *Palaeontology* 56, 475–486.
- Tütken, L., Dulai, A., Bitner, M. A., Vennemann, T. & Cooper, M. 2012: Geochemical composition of Neogene phosphatic brachiopods: implications for ancient environmental and marine conditions. *Palaeogeography, Palaeoclimatology, Palaeoecology* 326–328, 66–77.
- Ushatinskaya, G. T. 2008: Origin and dispersal of the earliest brachiopods. *Paleontological Journal* 42, 776–791.
- Ushatinskaya, G. T. 2012: The oldest lingulids of the Siberian Platform: microornamentation and shell structure. *Paleontological Journal* 46, 1298–1308.
- Ushatinskaya, G. T. & Korovnikov, I. V. 2014: Revision of the Early-Middle Cambrian Lingulida (Brachiopoda) from the Siberian Platform. *Paleontological Journal* 48, 26–40.
- Veiderma, M. & Knoubovets, R. 1972: An infrared spectroscopic study of phosphatic mineral in obolid phosphorite. *Eesti NSV Teaduste Akadeemia Toimetised. Keemia. Geoloogia* 21, 57–61, (in Russian with English summary).
- Watabe, N. & Pan, C.-M. 1984: Phosphatic shell formation in atremate brachiopods. *American Zoologist* 24, 977–985.
- Wenzel, B., Lécuyer, C. & Joachimski, M. M., 2000: Comparing oxygen isotope records of Silurian calcite and phosphate – $\delta^{18}\text{O}$ compositions of brachiopods and conodonts. *Geochimica et Cosmochimica Acta* 64, 1859–1872.
- Williams, A. 1997: Shell structure. In: Kaesler, R. L. (ed.) *Treatise on Invertebrate Paleontology. Part H, Brachiopoda Revised. Vol 1: Introduction*, 267–320. The Geological Society of America, Inc. and The University of Kansas. Boulder, Colorado and Lawrence, Kansas.
- Williams, A., Carlson, S. J. & Brunton, C. H. C. 2000: Linguliformea. In: Kaesler, R.L. (ed.) *Treatise on invertebrate paleontology Part H Brachiopoda Revised. Vol 2: Linguliformea, Craniiformea, and Rhynchonelliformea (part)*, 30–30. The Geological Society of America, Inc. and The University of Kansas. Boulder, Colorado and Lawrence, Kansas.
- Williams, A., Carlson, S. J., Howard, C., Brunton, C., Holmer, L. E. & Popov, L. 1996: A supra-ordinal classification of the Brachiopoda. *Philosophical Transactions of the Royal Society of London (series B)* 351, 1171–1193.
- Williams, A. & Cusack, M. 1997: Lingulid shell mediation in clay formation. *Lethaia* 29, 349–360.
- Williams, A. & Cusack, M. 1999: Evolution of a rhythmic lamination in the organo-phosphatic shells of brachiopods. *Journal of Structural Biology* 126, 227–240.
- Williams, A. & Cusack, M. 2007: Chemicostuctural diversity of the brachiopod shell. In: Selden, P. A. (ed.): *Treatise on Invertebrate Paleontology, Part H, Brachiopoda Revised, 6, Supplement*, 2396–2521. The Geological Society of America, Inc. and The University of Kansas. Boulder, Colorado and Lawrence, Kansas.
- Williams, A., Cusack, M. & Buckland, J. O. 1998: Chemicostuctural phylogeny of the discinoid brachiopod shell. *Philosophical Transactions of the Royal Society of London (series B)* 353, 2005–2038.
- Williams, A., Cusack, M. & Mackay, S. 1994: Collagenous chitinophosphatic shell of the brachiopod *Lingula*. *Philosophical Transactions of the Royal Society of London (series B)* 346, 223–266.
- Williams, A. & Holmer, L. E. 1992: Ornamentation and shell structure of acrotretoid brachiopods. *Palaeontology* 35, 657–692.

- Williams, A., Holmer, L. E. & Cusack, M. 2004: Chemico-structure of the organo-phosphatic shells of siphonotretide brachiopods. *Palaeontology* 47, 1313–1337.
- Williams, A., James, M. A., Emig, C. C., Macay, S. & Rhodes, M. C. 1997: Anatomy. In: Kaesler, R. L. (ed.) *Treatise on Invertebrate Paleontology. Part H, Brachiopoda Revised. Vol 1: Introduction*, 7–188. The Geological Society of America, Inc. and The University of Kansas. Boulder, Colorado and Lawrence, Kansas.
- Williams, A., Mackay, S. & Cusack, M. 1992: Structure of the organo-phosphatic shell of the brachiopod *Discina*. *Philosophical Transactions of the Royal Society of London (series B)* 337, 83–104.
- Yao, F., LeGeros, J. P. & LeGeros, R. Z. 2009: Simultaneous incorporation of carbonate and fluoride in synthetic apatites: effect on crystallographic and physico-chemical properties. *Acta Biomaterialia* 5, 2169–2177.
- Yi, H., Balan, E., Gervais, C., Segalen, L., Fayon, F., Roche, D., Person, A., Morin, G., Guillaumet, M., Blanchard, M., Lazzeri, M. & Babonneau, F. 2013: A carbonate-fluoride defect model for carbonate-rich fluorapatite. *American Mineralogist* 98, 1066–1069.

SUMMARY IN ESTONIAN

Vara-Paleosoikumi linguliformsete käsijalgsete kodade bakulaarne struktuur

Käsijalgsete ehk brahhiopoodid on rühm merelisi selgrootuid, kes on teada alates Kambriumi ajastust ning elavad ka tänapäeval. Käsijalgsete pehme keha on peidus kahe (kõhnmise ja selgmise) kojapoolme vahel. Kojapoolmed koosnevad paljudel käsijalgsetest kaltsiumkarbonaadist, kuid alamhõimkonda Linguliformea kuuluvatel nn linguliformsetel käsijalgsetel moodustab kojapoolmete mineraalosa kaltsiumfosfaat (apatiit). Kui kaltsiumkarbonaat on väga levinud tosematerjal mereliste selgrootute seas, siis apatiit on enam tuntud selgroogsete (sh inimese) luid ja hambaid moodustava mineraalina. Seos inimesega muudab skeletiapatiidi uurimise põnevaks, sest paralleele saab tõmmata iseendaga.

Linguliformsed brahhiopoodid sekreteerivad oma koda kihikaupa, kuid erinevate kihtide sekreteerimise viis on erinev. Selle tulemusena moodustavad kojapoolmeid vahelduvad kompaktsed (orgaanikavaesed) ning poorsed (orgaanikarikkamad) kihid. Kompaktsetes kihtides paiknevad apatiidikristallid tihedalt üksteise lähedal. Poorsetes kihtides moodustab apatiit enamasti keerulismaid struktuure, nt püstiseid jämedamaid postikesi või peenemaid, sageli võretaoliselt paigutatunud pulgataolisi moodustisi, mida kutsutakse baakulateks. Kojastruktuuride õige määramine fossiilsetes brahhiopoodikodades on tähtis, kuna tegemist on fülogeneetilisel olulise tunnusega (nt Cusack *et al.* 1999). Kuigi primaarsete struktuuride säilivust käsijalgsete kodades on püütud hinnata, võrreldes omavahel tänapäevaseid ja Karboni-ealisi *Lingula* kodasid (Cusack & Williams 1996), ilmneb struktuuride interpreteerimisel siiski ebakõlasid (nt Pettersson Stolk *et al.* 2010). Fossiliseerunud käsijalgsete kodade struktuuri tüüpi määramine ristlõikepinnal ei ole alati lihtne, sest mõnikord pole struktuurid säilinud või on hiljem tugevasti muutunud. Pulbristatud kodade röntgen-difraktsioon-uringute tulemused näitavad, et fossiilsed käsijalgsete koad sisaldavad mitut tüüpi apatiiti, mis tõenäoliselt on ka erineva tekkega (Nemliher *et al.* 2004, Cusack & Williams 2007). Kuna erinevate apatiidifaaside olemasolu oli kindlaks tehtud vaid pulbristatud kojamaterjalis (Nemliher *et al.* 2004), siis oli ebaselge, kuidas need faasid koad jaotuvad ning mille poolest nad üksteisest erinevad. Samuti ei mõistetud siiani kuigi hästi kodade surmajärgseid muutumisprotsesse (diageneetilisi muutusi). Lisaks struktuuriuringutele tekitab kojaapatiidi diageneetiliste muutuste mittemõistmine segadust ka paleokliima uuringutes (nt Lécuyer *et al.* 1996, 1998; Wenzel *et al.* 2000; Bassett *et al.* 2007), kus oleks oluline eristada looma eluajal kojaapatiiti salvestunud informatsiooni ning diageneetiliste muutuste tagajärgi.

Eelnevat arvesse võttes seati käesoleva töö eesmärgiks analüüsida käsijalgsete kodade bakulaarse struktuuri iseärasusi ja fossiliseerumisel aset leidnud diageneetiliste muutuste iseloomu, et selgitada võimaluste piires erinevate apatiidifaaside koostis ja levik koad. Püstitati eesmärk luua terviklik ettekujutus kojamaterjalis aset leidnud diageneetilistest muutustest, mille baasil tehtavad

järeldused saaksid senisest paremaks aluseks linguliformsete käsijalgsete süstemaatikale ning võimaldaksid senisest objektiivsemalt hinnata kojamaterjali kasutamise võimalusi paleoökoloogilistes ja paleokeskkonna uuringutes.

Antud doktoritööga seotud uuringud võib tinglikult jagada kaheks osaks. Olulise osa tööst moodustavad Kambriumi 3. (seni veel nimetamata) ajastiku *Obolus ruchini*, Furongi *Ungula inornata* ning Kesk-Devoni *Bicarinatina bicarinata* kodade murdepindade detailuuringud (Lang & Puura 2009, 2013; Lang *et al.* 2011). Töö teises osas kaardistati Furongi vanusega *Ungula ingraca* kodade keemilist koostist (Lang *et al.* 2015). *Ungula ingraca* kojad on üheks põhiliseks Eesti fosforiidilasundit moodustavaks komponendiks. Kõigile nimetatud liikidele on omane nn bakulaarne kojastruktuur, mille iseloomulikuks jooneks on apatiitsete pulgataoliste moodustiste, nn baakulate esinemine kompaksete kihtidega vahelduvates poorsemates (bakulaarsetes) kihtides (Holmer 1989). Kuigi käsijalgsete kodades võib esineda ka muid struktuuritüüpe (nt kolumnaarne, virgoosne), on bakulaarne struktuuritüüp ainus pika geoloogilise ajalooga tunnus, mis on teada alates Kambriumi 2. (seni veel nimetamata) ajastikust (Skovsted & Peel 2010) ning esineb samal ajal ka tänapäevaste linguliformsete käsijalgsete kodades.

Kojastruktuuri uurimiseks kasutati kodade töötlemata murdepindu, et vältida töötlemisest tulenevat võimalikku mõju habrastele kojastruktuuridele. Madalvaakumi skaneeriva elektronmikroskoopia (SEM) uuringute tulemused näitasid, et kodade murdepindadel nähtav struktuur võib varieeruda väga laiaades piirides ning ühes ja samas kajas võib esineda nii tüüpilisi baakulaid kui ka täiesti massiivseid piirkondi. Lisaks õnnestus kodade kõige alumistes (sisemistes) kihtides esmakordselt kirjeldada väga peeni, 100–200 nm diameetriga niitjaid moodustisi. Need, nn nanofiibrid, esinevad nii „Kesk-Kambriumi“ *O. ruchini*, Furongi *U. inornata* kui ka Kesk-Devoni *B. bicarinata* kojamaterjalis, tavaliselt sisemistes (nooremates) bakulaarsetes kihtides. Oma mõõdmetelt sarnanevad nad kõige enam tänapäevaste brahhiopoodide bakulaarset struktuuri kujundavate orgaaniliste niitjate moodustistega. Fiibrite kuju lubab oletada, et nad olid looma eluajal elastsed ja võisid painduda. Kõigest eelnevast tuleneb oletus, et leitud struktuurid kujutavad endast bakulaarse struktuuri orgaanilist raamistikku, mis on säilinud kiire varase fosfatiseerumise tulemusena. Perekondade *Obolus*, *Ungula* ja *Bicarinatina* liikide võrdlevad struktuuriuuringud näitavad, et baakulate suurus (diameeter) ja orientatsioon võib ka sama koja piires märkimisväärselt muutuda, samas kui nanofiibrid on neis kodades suhteliselt sarnaste parameetritega. See omakorda lubab oletada, et sarnaste parameetritega nanofiibrite olemasolu on bakulaarse struktuuritüübi oluline, iseloomulik tunnus. Nanofiibrite roll bakulaarse struktuuri kujundamisel on ilmne ning nende sarnane iseloom retsentsetes ja fossiilsetes kodades näitab, et linguliformsete käsijalgsete baakulate arengus ei ole Faneroosiumi vältel toimunud olulisi muutusi. Vähemalt Kambriumi 3. ajastikust peale on baakulad kujunenud samuti kui tänapäevalgi: baakula hakkab arenema nanofiibri ümber ning mõnikord haarab ühe suurema baakula areng mitu nanofiibrit.

Kodade keemilise koostise uuringud viidi läbi selleks, et lokaliseerida ja iseloomustada pulbristatud kojamaterjalis röntgendifraktsioonanalüüsi (XRD) tulemusena eristatud apatiidifaase (Nemliher *et al.* 2004) ning teha kindlaks, milliseid keemilisi muutusi toob kaasa bakulaarse kojastruktuuriga käsijalgsete diagenees ja millised piirkonnad võiksid kodades tõenäoliselt olla paremini säilinud. Uuritavaks materjaliks olid tugevalt mineraliseerunud *U. ingrica* kodade lihvitud ristlõikepinnad, mida uuriti energiadiispersiivse spektroskoopia (EDS) ja infrapunakaardistamise (ATR-FTIR) meetodil. Infrapunakaardistamist pole fossiilsete käsijalgsete puhul varem kasutatud. Kasutatud meetodite kombinatsioon võimaldas esmakordselt teha kindlaks erinevate apatiidifaaside paiknemise fossiilsetes brahhiopoodikodades ning iseloomustada faaside koostise erinevusi. Tulemustest ilmnes, et erinevate apatiidifaaside levik järgib *U. ingrica* koja struktuurset kihte – üks faas on seotud kompaktkihtide ning teine poorsete (bakulaarsete) kihtidega. Võrreldes faase nii omavahel kui ka tänapäevaste linguliformsete käsijalgsete kojaapatiidiga, selgus, et apatiidifaas kompaktkihtides sarnaneb nii oma võreparameetritelt, apatiidi kristallitide morfoloogialt kui ka karbonaatiooni ja fluoriidiooni sisalduselt tänapäevaste linguliformsete käsijalgsete kojaapatiidiga. Lisaks esineb kompaktkihtide apatiidil iseloomulik infrapunakiirguse neeldumismaksimum lainearvul $\sim 872\text{ cm}^{-1}$, mis on iseloomulik ka tänapäevase *Lingula* kojaapatiidile (LeGeros *et al.* 1985, Rohanizadeh & LeGeros 2007). See sarnasus lubab oletada, et kompaktkihtide apatiit võib kajastada Furongi ajastiku keskkonnaparameetreid, ehkki kationide asendumised selle apatiidifaasi kristallvõres viitavad teatavatele diagenetilistele muutustele.

Bakulaarsetes kihtides esinev apatiidifaas erineb kompaktkihtide faasist tunduvalt kõrgema karbonaat- ja fluoriidiooni sisalduse, madalama XRD võreparameetri a väärtuse ning apatiidikristallitide selgelt prismalise morfoloogia poolest. Lisaks esineb bakulaarsete kihtide apatiidil karbonaatiooni esinemisele viitav infrapunakiirguse neeldumismaksimum lainearvul 864 cm^{-1} , mida peetakse fossiliseerunud apatiitsetes skelettides diagenetiliste muutuste tunnuseks (Yi *et al.* 2013). Selle faasi päritolu pole aga antud doktoritöö uuringute alusel selge. Tegemist võib olla kas orgaanika fosfatiseerumisel, algse kojaapatiidi tugeval ümberkristalliseerumisel, orgaanika lagunemisel tekkiva sekundaarapatiidi ladestumisel või hoopis mitme protsessi koosmõjul moodustunud faasiga.

Struktuuri ja keemilise koostise muutuste alusel sai võimalikuks brahhiopoodide kojaapatiidi diageneesi üldistatud stsenaariumi kirjeldamine. Tulemustest ilmnes, et ka ühe kojapoolme piires võib struktuur varieeruda. Samal ajal kui mõnes kojapiirkonnas esineb nanofiibreid, võivad teised piirkonnad olla massiivsed. Selline struktuuri varieeruvus lubab oletada, et kodade kihilise ehituse, kihtide erineva paksuse ning orgaanikarikkuse tõttu kujunevad koja erinevates piirkondades erinevad diagenetilised tingimused. Seega on linguliformsete käsijalgsete koja diagenees oma olemuselt keeruline protsess, mille põhilisteks etappideks on 1) fosfatiseerumine, 2) kojaapatiidi stabiliseerumine, 3) apatiidi morfoloogia muutused ja 4) koja massiivseks muutumine sekun-

daarse apatiidi ladestumise tõttu. Diageneesi kõige varajasemas staadiumis toimub koja struktuuris esineva orgaanika valikuline fosfatiseerumine, mille tõttu võivad säilida nanofiibrid. Orgaanika lagunedes muutub bioapatiidi kristalliite ümbritsev keskkond ning uue tasakaalu kujunemise käigus leiab aset kristalliitide stabiliseerumine sõltuvalt sellest, milline diageneetiline keskkond antud kojapiirkonnas on kujunenud. Kompaktkihtides on apatiidi kristalliidid tihedalt üksteise lähedal, orgaanikat esineb vähem ning seetõttu võib säilida nii algne kristalliitide morfoloogia kui ka primaarsele lähedane keemiline koostis. Poorsetes bakulaarsetes kihtides on aga orgaanikat rohkem ning pH muutumisel ja üleküllastuse tekkimisel jätkub prismadeks ümber kristalliseerunud apatiidi muutumine ja moodustuma hakkavad liivakellakujulised ning sfääruliitsed agregaadid. Sobivate tingimuste püsimisel hakkavad need agregaadid kasvama ning selle käigus võivad algsete baakulate mõõtmed märkimisväärselt muutuda, kuni baakulate sulandumise ning struktuuri täieliku ühtlustumiseni. On tõenäoline, et selle protsessi käigus lisandub primaarsele kojaapatiidile sekundaarset (autigeenset) apatiiti, mis võib olla bakteriaalset päritolu. Orgaanika bakteriaalse lagundamise tulemusel tekkiva apatiidifaasi isotoopkoostis võib aga oluliselt erineda primaarse apatiidi omast (Goldhammer *et al.* 2011) ning see muudab küsitavaks bakulaarsetes kihtides oleva apatiidi kasutamise paleokeskkonna interpreteerimisel.

Kuna ka Eesti fosforiid koosneb linguliformsete käsijalgsete (sh nt *U. ingraca* ja *U. inornata*) kojapoolmetest, aitavad kodade keemilise koostise ning mikrostruktuuri uuringud tulevikus paremini mõista ka fosforiidi omadusi ning kujunemise põhjusi. Nende uuringute tulemused võivad tulevikus omakorda olla olulised fosforiidi tehnoloogiliste omaduste ning kaevandamisega seotud keskkonnaprobleemide analüüsimisel.

PUBLICATIONS

CURRICULUM VITAE

Name: Liisa Lang
Date of birth: November 1, 1983
Address: Department of Geology, University of Tartu,
Ravila 14a, 50411 Tartu, Estonia
Contact: Phone: +372 737 6686
Fax: +372 737 5836
E-mail: liisa.lang@gmail.com; liisa.lang@ut.ee

Education:
2007–2015 PhD Candidate in Geology: University of Tartu, Department of Geology (Supervisors: Prof. Tõnu Meidla and PhD Ivar Puura)
2005–2007 MSc in Geology (*cum laude*): University of Tartu, Department of Geology (Supervisor: PhD Ivar Puura)
2002–2005 BSc in Geology: University of Tartu, Department of Geology (Supervisor: PhD Ivar Puura)

Professional employment:

2013–... specialist of palaeontology, University of Tartu, Department of Geology
2012–2013 laboratory assistant (palaeontology), University of Tartu, Department of Geology
2011–2012 specialist on digital data (palaeontology), University of Tartu, Natural History Museum
2008–2010 project manager, University of Tartu
2006–2007 senior specialist, Estonian Land Board

Research activity:

Research interests: palaeontology, apatite, brachiopods, diagenesis

Grants and scholarships:

2012– Archimedes Foundation (Kristjan Jaak programme)
2010– Doctoral School of Earth Sciences and Ecology
2010– Archimedes Foundation (Kristjan Jaak programme)
2010– Alwyn Williams Fund
2009– Archimedes Foundation (Kristjan Jaak programme)

Research training:

2010– EDIT-DEST Modern Taxonomy programme 2010–2011 course „Biological Nomenclature“ at the Natural History Museum in Paris, France. Advisor: Dr. Alain Dubois.

Publications:

Scientific publications:

- Lang, L.**, Kirsimäe, K., Vahur, S. 2015: Diagenetic fate of bioapatite in linguliform brachiopods: multiple apatite phases in shells of Cambrian lingulate brachiopod *Ungula ingraca* (Eichwald). *Lethaia* (in press).
- Lang, L.**, Puura, I. 2013: Phosphatized organic nanostructures in the Cambrian linguloid brachiopod *Ungula inornata* (Mickwitz). *Estonian Journal of Earth Sciences*, 62(3), 121–130.
- Lang, L.**, Uibopuu, E., Puura, I. 2011: Nanostructures in Palaeozoic linguloid brachiopods. *Memoirs of the Association of Australasian Palaeontologists*, 41, 359–366.
- Lang, L.**, Puura, I. 2009: Systematic position, distribution, and shell structure of the Devonian linguloid brachiopod *Bicarinatina bicarinata* (Kutorga, 1837). *Estonian Journal of Earth Sciences*, 58(1), 63–70.

Popular scientific publications:

- Lang, L.** 2014: Kaltsiumfosfaatsed kivistised: pilk käsijalgse koja sisse. Lang, L.; Truuver, K.; Post, T. (eds.). Fosfor – aegade algusest tänapäevani. *Schola Geologica X*, 42–47. Tartu: Estonian Naturalists Society.
- Puura, I., **Lang, L.** 2011: Fosforiit elektronmikroskoobi all. *Eesti Loodus*, 10, 14–17.
- Lang, L.** (2010). Skeletiteke. Preeden, U.; Laumets, L. (eds.). Globaalsed muutused. *Schola Geologica VI*, 121–125. Tartu: Estonian Naturalists Society.
- Lang, L.**, Laumets, L., Meidla, T. 2009: Charles Darwin kui geoloog. *Eesti Loodus*, 2, 14–17.
- Lang, L.**, Puura, I. 2009: Biomineraalid me ümber ja me sees. Verš, E., Amon, L.; Laumets, L. (eds.). Piirideta Geoloogia, *Schola Geologica V*, 13–19. Tartu: Estonian Naturalists Society.
- Lang, L.**, Laumets, L. 2009: Charles Lyell: tänapäev on võti mineviku mõistmiseks. Rohtmets, I., Kukk, T. (eds.). *Lehed ja tähed: Vaim ja aeg*, 86–93. Tallinn: Tallinna Raamatutrükikoda.

ELULOOKIRJELDUS

- Nimi:** Liisa Lang
Sünniaeg: 1. november, 1983
Aadress: Geoloogia osakond, Tartu Ülikool, Ravila 14a, 50411 Tartu, Eesti
Kontakt: Tel: +372 737 6686
Faks: +372 737 5836
E-post: liisa.lang@gmail.com; liisa.lang@ut.ee
- Haridus:**
2007–2015 geoloogiadoktorant: Tartu Ülikool, geoloogia osakond (juhendajad: prof. Tõnu Meidla, PhD Ivar Puura)
2005–2007 magistrikraad geoloogias (*cum laude*): Tartu Ülikool, geoloogia osakond (juhendaja: PhD Ivar Puura)
2002–2005 bakalaureusekraad geoloogias: Tartu Ülikool, geoloogia osakond (juhendaja: PhD Ivar Puura)
- Teenistuskäik:**
2013–... paleontoloogia spetsialist, Tartu Ülikool, geoloogia osakond
2012–2013 laborant (paleontoloogia), Tartu Ülikool, geoloogia osakond
2011–2012 digiandmete spetsialist (paleontoloogia), Tartu Ülikooli Loodusmuuseum
2008–2010 projektijuht, Tartu Ülikool
2006–2007 vanemspetsialist, Maa-amet
- Teadustegevus:**
Teadustöö põhisuunad: paleontoloogia, apatiit, käsijalgsed, diagenees
- Saadud uurimistoetused ja stipendiumid:**
2012– SA Archimedes (Kristjan Jaagu programm)
2010– Maateaduste ja ökoloogia doktorikool
2010– SA Archimedes (Kristjan Jaagu programm)
2010– Sir Alwyn Williamsi Fond
2009– SA Archimedes (Kristjan Jaagu programm)
- Erialane enesetäiendus:**
2010– EDIT-DEST tänapäevase taksonoomia programmi „Bioloogilise nomenklatuuri“ kursus Prantsusmaal Pariisi Loodusmuuseumis. Juhendaja dr Alain Dubois.

Publikatsioonid:

Teaduslikud publikatsioonid:

- Lang, L.**, Kirsimäe, K., Vahur, S. 2015: Diagenetic fate of bioapatite in linguliform brachiopods: multiple apatite phases in shells of Cambrian lingulate brachiopod *Ungula ingraca* (Eichwald). *Lethaia* (avaldamisel).
- Lang, L.**, Puura, I. 2013: Phosphatized organic nanostructures in the Cambrian linguloid brachiopod *Ungula inornata* (Mickwitz). *Estonian Journal of Earth Sciences*, 62(3), 121–130.
- Lang, L.**, Uibopuu, E., Puura, I. 2011: Nanostructures in Palaeozoic linguloid brachiopods. *Memoirs of the Association of Australasian Palaeontologists*, 41, 359–366.
- Lang, L.**, Puura, I. 2009: Systematic position, distribution, and shell structure of the Devonian linguloid brachiopod *Bicarinatina bicarinata* (Kutorga, 1837). *Estonian Journal of Earth Sciences*, 58(1), 63–70.

Populaarteaduslikud publikatsioonid:

- Lang, L.** 2014: Kaltsiumfosfaatsed kivistised: pilk käsijalgse koja sisse. Lang, L.; Truuver, K.; Post, T. (toim.). Fosfor – aegade algusest tänapäevani. *Schola Geologica X*, 42–47. Tartu: Eesti Looduseuurijate Selts.
- Puura, I., **Lang, L.** 2011: Fosforiit elektronmikroskoobi all. *Eesti Loodus*, 10, 14–17.
- Lang, L.** (2010). Skeletiteke. Preeden, U.; Laumets, L. (toim.). Globaalsed muutused. *Schola Geologica VI*, 121–125. Tartu: Eesti Looduseuurijate Selts.
- Lang, L.**, Laumets, L., Meidla, T. 2009: Charles Darwin kui geoloog. *Eesti Loodus*, 2, 14–17.
- Lang, L.**, Puura, I. 2009: Biomineraalid me ümber ja me sees. Verš, E., Amon, L.; Laumets, L. (toim.). Piirideta Geoloogia, *Schola Geologica V*, 13–19. Tartu: Eesti Looduseuurijate Selts.
- Lang, L.**, Laumets, L. 2009: Charles Lyell: tänapäev on võti mineviku mõistmiseks. Rohtmets, I., Kukk, T. (toim.). *Lehed ja tähed: Vaim ja aeg*, 86–93. Tallinn: Tallinna Raamatutrükikoda.

DISSERTATIONES GEOLOGICAE UNIVERSITATIS TARTUENSIS

1. **Пэп Мянник.** Конодонты в верхнеордовикских и нижнесилурийских отложениях Эстонии. Тарту, 1992, 355 с.
2. **Elvi Tavast.** Fennoskandia kilbi lõunanõlva ja sellega piirnevate alade aluspõhja reljeef. Tartu, 1992, 357 lk.
3. **Kaarel Orviku.** Characterisation and evolution of Estonian seashores. Tartu, 1992, 19 p.
4. **Анатолий Молодьков.** ЭПР-анализ скелетного вещества моллюсков в хроностратиграфических исследованиях позднего кайнозоя. Тарту, 1992, 33 с.
5. **Jaan Lutt.** Late- and postglacial deposits on the Estonian shelf. Tartu, 1993, 31 p.
6. **Reet Karukäpp.** Gotiglatsiaalne morfogenees Skandinaavia mandriliustiku kagusektoris. Tartu, 1997, 181 p.
7. **Argo Jõelett.** Geothermal studies of the Precambrian basement and Phanerozoic sedimentary cover in Estonia and Finland. Tartu, 1998, 125 p.
8. **Jüri Nemliher.** Mineralogy of Phanerozoic skeletal and sedimentary apatites: an XRD study. Tartu, 1999, 134 p.
9. **Kalle Kirsimäe.** Clay mineral diagenesis on the Lower Cambrian “Blue Clay” in the northern part of the Baltic Paleobasin. Tartu, 1999, 113 p.
10. **Jüri Plado.** Gravity and magnetic signatures of meteorite impact structures. Tartu, 2000, 87 p.
11. **Olev Vinn.** Morphogenesis and phylogenetic relationships of Clitambonitidines, Ordovician Brachiopods. Tartu, 2001, 127 p.
12. **Leho Ainsaar.** The middle Caradoc facies and faunal turnover in the late Ordovician Baltoscandian palaeobasin: sedimentological and carbon isotope aspects. Tartu, 2001, 109 p.
13. **Oive Tinn.** Early Ostracode evolution and Palaeoenvironmental application in the Ordovician of Baltoscandia. Tartu, 2002, 145 p.
14. **Maris Rattas.** Subglacial environments in the formation of drumlins — The case of the Saadjärve Drumlin Field, Estonia. Tartu, 2004, 117 p.
15. **Ene Kadastik.** Upper-Pleistocene stratigraphy and deglaciation history in northwestern Estonia. Tartu, 2004, 129 p.
16. **Helje Pärnaste.** Early Ordovician trilobites of suborder Cheirurina in Estonia and NW Russia: systematics, evolution and distribution. Tartu, 2004, 138 p.
17. **Mari-Ann Mõtus.** Silurian (Llandovery-Wenlock) tabulate corals of Baltoscandia: taxonomy, palaeoecology, distribution. Tartu, 2005, 167 p.
18. **Alar Rosentau.** Development of proglacial lakes in Estonia. Tartu, 2006, 114 p.
19. **Evelin Verš.** Development of impact-induced hydrothermal system at Kärddla impact structure. Tartu, 2006, 96 p.

20. **Sigitas Radzevičius.** The genus *Pristiograptus* in Wenlock of East Baltic and the Holy Cross Mountains. Tartu, 2007, 133 p.
21. **Andres Marandi.** Natural chemical composition of groundwater as a basis for groundwater management in the Cambrian-Vendian aquifer system in Estonia. Tartu, 2007, 116 p.
22. **Eve Niinemets.** Vegetation and land-use history of the Haanja Heights (SE-Estonia) during the Holocene. Tartu, 2008, 146 p.
23. **Kalle-Mart Suuroja.** Geology and lithology of the early Palaeozoic marine impact structures Kärddla and Neugrund (Estonia). Tartu, 2008, 234 p.
24. **Rutt Hints.** Early diagenesis of Ordovician and Silurian Bentonites in the Northern Baltic Palaeobasin. Tartu, 2009, 90 p.
25. **Peeter Somelar.** Illitization of K-bentonites in the Baltic Basin. Tartu, 2009, 118 p.
26. **Ulla Preeden.** Remagnetizations in sedimentary rocks of Estonia and shear and fault zone rocks of southern Finland. Tartu, 2009, 121 p.
27. **Kati Tänavsuu-Milkeviciene.** Transgressive to regressive turnaround in the Middle Devonian Baltic Basin. Tartu, 2009, 106 p.
28. **Valle Raidla.** Chemical and isotope evolution of groundwater in the Cambrian-Vendian aquifer system in Estonia. Tartu, 2010, 134 p.
29. **Kadri Sohar.** Quaternary ostracods from Estonia and their application in palaeoenvironmental reconstruction. Tartu, 2010, 140 p.
30. **Kristjan Urtson.** Stepwise melt transport and accumulation: analogue and numerical modelling approach. Tartu, 2011, 83 p.
31. **Marko Kohv.** Landslides in clayey soils of western Estonia. Tartu, 2011, 116 p.
32. **Nele Muttik.** Post-impact alteration of impactites: Ries crater, Germany. Tartu, 2011, 78 p.
33. **Annette Sedman.** Strength and self-cementing properties of oil shale retorting wastes. Tartu, 2013, 82 p.
34. **Arkady Tsyrunnikov.** Complex seismo-acoustic and lithological study of the Lateglacial and postglacial sediments northern Gulf of Riga, eastern branch of the central Baltic Sea. Tartu, 2013, 102 p.
35. **Marge Uppin.** Geological sources and hydrochemistry of fluoride and boron in Silurian-Ordovician aquifer system. Tartu, 2013, 86 p.
36. **Peeter Talviste.** Temporal changes in weak natural and artificial soils – influence on geotechnical characteristics. Tartu, 2014, 204 p.
37. **Katrin Lasberg.** Chronology of the Weichselian Glaciation in the south-eastern sector of the Scandinavian Ice Sheet. Tartu, 2014, 100 p.
38. **Sirle Liivamägi.** Neoproterozoic Baltic paleosol: geology and paleoenvironmental interpretation. Tartu, 2015, 94 p.
39. **Lauri Joosu.** Petrography and the rare earth element composition of apatite in 2 Ga Onega and Pechenga basins, Russia: the environmental settings for phosphogenesis. Tartu, 2015, 139 p.